Biochemical Pharmacology 155 (2018) 547–561

Contents lists available at ScienceDirect

Biochemical Pharmacology

journal homepage: www.elsevier.com/locate/biochempharm

Strategies and limitations associated with in vitro characterization of vitamin D receptor activators

Paola Bukuroshi[a], Hiroshi Saitoh[b], Lilia Magomedova[a], Carolyn L. Cummins[a], Edwin C. Chow[a], Albert P. Li[c], K. Sandy Pang[a,*]

[a] Department of Pharmaceutical Sciences, Leslie Dan Faculty of Pharmacy, University of Toronto, Toronto, Ontario, Canada
[b] Teijin Pharma Inc., 3-2, Asahigaoka 4-chome, Hino, Tokyo 191-8512, Japan
[c] In Vitro ADMET Laboratories, Columbia, MD 21045, USA

ARTICLE INFO

Keywords:
Vitamin D receptor activators
Cell-based assays
Strategy and characterization
Activation enzymes
Inhibition

ABSTRACT

In vitro cell-based assays are common screening tools used for the identification of new VDR ligands. For 25-hydroxyvitamin D_3 [25(OH)D_3] and 1α-hydroxyvitamin D_3 [1α(OH)D_3], protein expressions of CYP2R1 and CYP27B1, respectively, that form the active 1α,25-dihydroxyvitamin D_3 [1,25(OH)$_2$$D_3$] ligand were detected in human embryonic kidney (HEK293) cells expressing the GAL4-hVDR, the human brain microvessel endothelial (hCMEC/D3) and adenocarcinoma colonic (Caco-2) cells. The impact of bioactivation enzymes was shown upon the addition of ketoconazole (10 μM KTZ), a pan-CYP inhibitor, which reduced the apparent potency of 25(OH)D_3 and increased the EC_{50} from 272 to 608 nM in HEK293 cells. EIA assays verified that 1,25(OH)$_2$$D_3$ was formed and contributed to VDR activity independently of its precursors. In hCMEC/D3 cells where enzyme protein levels were lowest, changes in MDR1/P-gp expression with KTZ were minimal. In Caco-2 cells, the induction of TRPV6 (calcium channel), CYP24A1, CYP3A4, OATP1A2 and MDR1 mRNA expression was 1,25(OH)$_2$$D_3$ > 1α(OH)D_3 > 25(OH)D_3, with the magnitude of change being blunted by KTZ. Upon inclusion of KTZ in the cell-based assays, high transcriptional activities were observed for synthetic VDR activators from Teijin Pharma. Cyclopentanone derivatives: TPD-003, TPD-005, TPD-006, TPD-008 and TPD-009 (EC_{50}s 0.06 to 67 nM, unchanged with KTZ) were found more potent over straight chain and lactone derivatives (antagonists). Most TPD compounds activated OATP1A2, CYP24A1, CYP3A4, and MDR1 (28–67%) and TRPV6 transcriptionally in Caco-2 cells. The results identified that cell-based assays with added KTZ could accurately identify new VDR activators, although these may be hypercalcemic with strong TRPV6 inducing properties.

1. Introduction

1α,25-Dihydroxyvitamin D_3 [1,25(OH)$_2$$D_3$], the active natural and endogenous ligand of the vitamin D receptor (VDR), is formed via the sequential hydroxylation of vitamin D_3, first in the liver via the 25-hydroxylases (microsomal CYP2R1 or mitochondrial CYP27A1), converting vitamin D_3 to 25-hydroxyvitamin D_3 [25(OH)D_3] [1–3], then in the kidney via 1α-hydroxylase (CYP27B1) to form active 1,25(OH)$_2$$D_3$ [4,5]. Thereafter, 1,25(OH)$_2$$D_3$ is inactivated by mitochondrial 24-hydroxylase, CYP24A1, to form 1,24,25-calcitroic acid [6]. The VDR is known to regulate plasma calcium via the absorptive calcium channels, mostly by TRPV6 in intestine and less by TRPV5 and TRPV6 in kidney [7,8]. Furthermore, VDR is an important regulator of drug transporters and enzymes, including the P-glycoprotein (P-gp), MRP2 and MRP4 [9], organic anion transporting polypeptide 1A2 (OATP1A2) [10], renal OAT3 [11,12]. sulfotransferase 2A1 (SULT2A1) [13], and cytochrome P450 3A4 (CYP3A4) [14].

25(OH)D_3 is a precursor of 1,25(OH)$_2$$D_3$ that is bioacitvated specifically by the 1α-hydroxylase, CYP27B1, of K_m of 2.7 μM in mouse and man [15], and directly binds and activates the VDR although with much lower affinity compared to 1,25(OH)$_2$$D_3$. In humans, 25(OH)$D_3$ is metabolized to inactive metabolites, to a great extent to its sulfate conjugate via SULT2A1 [16,17], then by CYP24A1 to 24,25(OH)$_2$$D_3$ [18], to glucuronides via UGT1A4/UGT1A3 [19], and 4β- and 4α-25(OH)$_2$$D_3$ via CYP3A4 in lesser extents [20]. In rats, treatment with increasing doses of 25(OH)D_3 maintained constant 1,25(OH)$_2$$D_3$ serum levels but decreased kidney rCyp27b1 and increased rCyp24a1, suggesting VDR activities attributed to the active metabolite, 1,25(OH)$_2$$D_3$ [21]. In *Cyp27b1*-knockout mice, where the conversion of 25(OH)D_3 to 1,25(OH)$_2$$D_3$ is absent, 25(OH)D_3 was found to increase plasma calcium, suggesting that 25(OH)D_3 has activity of its own (5).

* Corresponding author at: Leslie Dan Faculty of Pharmacy, University of Toronto, 144 College Street, Toronto, Ontario M5S 3M2, Canada.
E-mail address: ks.pang@utoronto.ca (K.S. Pang).

https://doi.org/10.1016/j.bcp.2018.07.015
Received 1 May 2018; Accepted 14 July 2018
Available online 18 July 2018
0006-2952/

By contrast, 1α(OH)D_3 is a synthetic analog that is converted to 1,25(OH)$_2D_3$ by liver mitochondrial CYP27A1 and microsomal CYP2R1 enzymes [22] of K_m of 9.6 μM [23], but there is little or no conversion by CYP24A1 to 1,24(OH)$_2D_3$ [24]. When mice were treated in vivo with equimolar doses of 1α(OH)D_3 and 1,25(OH)$_2D_3$, 1α(OH)D_3 caused a higher extent of hypercalcemia [25]. Along the same lines, Fan et al. reported that treatment of Caco-2 cells with 1α(OH)D_3 but not 25(OH)D_3 led to increased protein expression levels of P-gp, MRP2, MRP3 and MRP4 [26]. In mice in vivo, treatment with 1α(OH)D_3 increased liver mCyp24a1 and mCyp7a1 as well as kidney mCyp24a1, mMrp2, mMrp3 and mMrp4 levels [27], and 1α(OH)D_3 was identified to be more active than 25(OH)D_3 in the lowering of cholesterol in hypercholesterolemic C57BL/6 mice [28].

Since 1,25(OH)$_2D_3$ activates brain MDR1 and reduces toxic brain amyloid-β peptides that are P-gp substrates [29], we are interested to continue our search for vitamin D analogs that would stimulate human brain MDR1 without over-stimulation of intestinal calcium uptake by the calcium channel, TRPV6, in avoidance of hypercalcemia. The Teijin (TPD) compounds represent a group of synthetic vitamin D receptor activators (VDRAs) that are used to test for the VDR-mediated activities. With the exception of TPD-014 (also known as TEI-9647), a derivative of the naturally occurring 1,25(OH)$_2D_3$ metabolite, 1,25(OH)$_2D_3$-26,23-lactone is a known antagonist [30,31], initially isolated from dog serum after 2 doses of 1.5 mg/dog of 1,25(OH)$_2D_3$ [32], few of the other Teijin compounds have been characterized for their VDR activity.

In this communication, we described a series of in vitro tests that may be applicable for the screening of potential VDRAs for their desirable and undesirable properties, based on findings from 1,25(OH)$_2D_3$ and its precursors/analogs, 25(OH)D_3 and 1α(OH)D_3, of known VDR activity [25,26,28]. Using the GAL4 luciferase reporter ligand screening assay in human embryonic kidney (HEK293) cells, we noted a discrepancy in the apparent EC_{50} estimates that were determined in the absence and presence of the P450 inhibitor, ketoconazole (KTZ, 10 μM) for 25(OH)D_3. Further probing revealed an abundance of CYP2R1 and CYP27B1 in HEK293 cells, enzymes that would activate these precursors and invalidate the potency/activity estimates. The formation of 1,25(OH)$_2D_3$ in turn would inhibit CYP27B1 and stimulate its own degradation by induction of CYP24A1 [33]. The same comment applies to other cell-based systems: hCMEC/D3 and Caco-2 cells, found to contain much lesser protein expressions of the enzymes. Thus, the in vitro assays were modified by inclusion of KTZ to render more accurate EC_{50} measurements of the intact VDRAs from Teijin Pharma in the GAL4 luciferase assays, as well as transcriptional activities of the intact compounds on VDR target gene expression: MDR1/P-gp in hCMEC/D3 cells and TRPV6 in Caco-2 cells.

2. Materials and methods

2.1. Reagents

1,25(OH)$_2D_3$, 25(OH)D_3, and 1α(OH)D_3 in powder forms were obtained from Sigma-Aldrich (St. Louis, MO). Anhydrous ethanol was used to dissolve the compounds, and the resulting concentrations were measured spectrophotometrically at 265 nm. Teijin compounds (TPD-001 to TPD-014 and TPD-090) were provided by Teijin Pharma Company (Japan). All dilutions of the compounds were made in ethanol. High glucose Dulbecco's Modified Eagle's Medium (DMEM), penicillin/streptomycin (P/S), 0.25% trypsin-EDTA solution, Dulbecco's Phosphate Buffered Saline (PBS), and non-essential amino acids were all obtained from Sigma-Aldrich (St. Louis, MO). Fetal bovine serum (FBS), charcoal stripped FBS (cs-FBS), and heat-inactivated FBS were purchased from Invitrogen (Carlsbad, CA). Basal endothelial media EGM-2 and growth factors were procured from Lonza (Walkersville, MD). Tissue culture plates were obtained from BD Bioscience (Mississauga, ON). TRIzol, chloroform, 2-propanol, and ketoconazole were obtained from Sigma-Aldrich (St. Louis, MO). Antibodies against GAPDH (ab8245), CYP2R1 (ab137634) and CYP27B1 (ab95047) were purchased from Abcam (Cambridge, MA). The P-gp antibody was obtained from ID Labs Inc. (London, ON) and CYP24 (C-18) from Santa Cruz Biotechnology (Dallas, TX), whereas the secondary anti-mouse, anti-rabbit and anti-goat antibodies were purchased from Bio-Rad (Mississauga, ON). The Pierce LDH cytotoxicity assay kit, purchased from Life Technologies (Burlington, ON), was used to test for cell toxicity of various concentrations of KTZ (up to 25 μM). The enzyme-immunoassay (EIA) kit for the determination of 1,25(OH)$_2D_3$ was purchased from ImmunoDiagnostic Systems (Gaithersburg, MD). All other reagents were obtained from Sigma-Aldrich, Life Technologies or Bioshop Canada Inc. (Burlington, ON).

2.2. Cell lines and culture conditions

2.2.1. HEK293 cells

Human embryonic kidney cells (HEK293) were maintained in high-glucose Dulbecco's modified Eagle medium (DMEM) supplemented with 10% FBS and penicillin/streptomycin (stock diluted to 1 × P/S) at 37 °C in the 5% CO_2 incubator. For the transfection assays, HEK293 cells were first seeded onto clear bottom 96-well plates at 40,000 cells/well in 100 μl DMEM, supplemented with 10% cs-FBS in the evening (Day 1). The following morning (Day 2), cells were transfected upon addition of the DNA of interest and calcium phosphate in 10 μl, according to Adachi et al. [34]. The total amount of plasmid DNA (150 ng) consisted of 50 ng of UAS-luciferase reporter, 20 ng β-galactosidase, 15 ng GAL4-DNA binding domain for VDR (GAL4-hVDR) or the CMX control plasmid, and 65 ng pGEM filler plasmid per well; the plasmids are kind gifts from Dr. David J. Mangelsdorf, University of Texas Southwestern Medical Center, Dallas, TX). Six to eight hours after transfection, cells were treated with vehicle (0.1% ethanol) or ligand (concentrations of 0.01–250 nM) of 1α(OH)D_3, 25(OH)D_3, and 1,25(OH)$_2D_3$ in 40 μl of treatment media for Set I, and the Teijin analogs TPD-001 – TPD-014, TPD-090 in 0.1% ethanol in DMEM media supplemented with 10% cs-FBS, in triplicate, in Set II. For the P450 inhibition studies, 10 μM KTZ was co-incubated with the ligands. At 14–16 h after treatment with ligand (Day 3), cells were examined for morphological changes before harvest. The medium was removed and 50 μl luciferase buffer (10X Core, 10X Triton, 10 mM luciferin, 0.1 M ATP, 50 mM CoA and β-mercaptoethanol) was added to cells. After covering the plate with foil, the plate was shaken to dislodge/dissociate the cells before the luciferase signal was read. Then 125 μl β-GAL buffer (ONPG and β-mercaptoethanol) was added and the "time" for color change in a 37 °C incubator (< 10 min at 37 °C) was recorded prior to reading of the β-galactosidase activities, monitored to correct for transfection efficiency with a microplate reader. The relative luciferase unit (RLU) was calculated as (luciferase light units/β-galactosidase)* "time". All transfections were performed in triplicates and repeated three separate times. The EC_{50} was estimated by fitting the data to a 4-parameter logistic model using GraphPad Prism. To assess whether the agonist properties of Teijin compounds were VDR specific, a panel of plasmids for other GAL4-nuclear receptors: LXRα/β, FXR, GR, MR, PPARα/β/γ, and PR (also from Dr. Mangelsdorf) was tested using a similar luciferase reporter assay. Also, the interaction between 10 nM 1,25(OH)$_2D_3$, and 25(OH)D_3 or 1α(OH)D_3 (0.1 to 500 nM) was examined in the transfection system in the presence of 10 μM KTZ, in triplicate.

2.2.2. 1,25(OH)$_2D_3$ formation from 25(OH)D_3 or 1α(OH)D_3 in HEK293 cells

HEK293 cells, which were plated in 96-well plates in the usual manner as for transfections, were incubated for 14–16 h with 0.1% ethanol (vehicle control), 100 nM of 25(OH)D_3, 1α(OH)D_3, 1,25(OH)$_2D_3$ or vitamin D_3 (vehicle control) in 150 μl treatment buffer. Then cells were harvested after 16 h of incubation. The cells, together with the incubation medium, were sonicated then centrifuged to obtain total cell homogenate. One milliliter of the pooled homogenate was used for extraction as described previously [35]. The final extract was dried via N_2 gas and reconstituted in blank

stripped human serum (200 µl), as previously described, vortexed and spun via a filter tube (Pall Nanosep 0.2 µm centrifugal device from Millipore Sigma, Etobicoke, ON) for debris removal, and the resulting solution was transferred to a new tube [36]. Prior to $1,25(OH)_2D_3$ measurement, serial dilution of the sample was conducted with blank stripped human serum: the reconstituted extracts of the 100 nM $1,25(OH)_2D_3$-treated samples were diluted with blank stripped human serum twice (1:25 v/v) for a total of 625-fold, whereas those for $25(OH)D_3$ or $1\alpha(OH)D_3$ and VDRAs samples were diluted up to 2-fold. A total of 150 µl of the final solution was used for $1,25(OH)_2D_3$ measurement with the EIA kit according to the Manufacturer's protocol [35,36]. The measured $1,25(OH)_2D_3$ concentration for sample was corrected by the factor, (200/150), for the volume prepared vs. the volume used for extraction and measurements.

2.2.3. hCMEC/D3 cells

The human brain microvessel endothelial cells (hCMEC/D3, obtained originally from Dr. Pierre Olivier Courand, Inserm, Institut Cochin, Paris, France via Dr. Reina Bendayan, University of Toronto), were maintained in basal EGM-2 endothelial media supplemented with vascular endothelial growth factor, insulin-like growth factor 1, epidermal growth factor, fibroblast growth factor, hydrocortisone, ascorbic acid, heparin, gentamycin and 5% of heat-inactivated FBS [37]. Cells were grown on plates coated with rat-tail collagen type I. After reaching 80% confluency (2 days after seeding, passage 28–33, and plated at a density of 33,000 cells/cm^2), cells were incubated for the next 3 days with 0.1% ethanol (vehicle) or 100 nM $25(OH)D_3$, $1\alpha(OH)D_3$, $1,25(OH)_2D_3$, or the Teijin analogs TPD-001 to TPD-014, TPD-090, in triplicate. Media was changed every other day for non-treatment days, and daily for treatment days.

2.2.4. Caco-2 cells

The adenocarcinoma cells (Caco-2) were maintained in high-glucose Dulbecco's modified Eagle medium supplemented with 10% FBS, 1% non-essential amino acids and 1× P/S at 37 °C in 5% CO_2 and cells were grown for a total of 21 days [2]). Caco-2 cells (passage 18–38, plated at a density of 25,000 cells/cm^2) were incubated with the vitamin D_3 precursors or activators: 100 nM of $1\alpha(OH)D_3$ and $25(OH)D_3$, $1,25(OH)_2D_3$, and the Teijin analogs TPD-001 – TPD-014, TPD-090, in the presence or absence of 10 µM KTZ, during the last 3 days of the 21-day incubation period, in triplicate. The concentration of 10 µM KTZ was found to be non-toxic in cells in preliminary experiments according to the LDH assay; the concentration of 25 µM KTZ, however, was found toxic (data not shown). The medium was changed every other day for non-treatment days, and daily during treatment days.

2.3. Real time quantitative PCR (qPCR)

Total RNA was extracted from cells using the TRIzol, and 1.5 µg of the RNA was converted to cDNA using the High Capacity Reverse Transcription System (Applied Biosystems), followed by qPCR using SYBR Green detection system [25,26,36]. The mRNA expression levels of genes of interest were then normalized to that of the housekeeping gene, GAPDH, and were calculated using the $2^{-\Delta\Delta Ct}$ method. The qPCR reactions were performed on an ABI 7500 machine in a 96-well plate format. The human primers used are summarized in Table 1.

2.4. Western blotting

Following the treatment of cells (HEK293, hCMEC/D3, and Caco-2), cell medium was gently aspirated after washing each well with PBS. Then the content of the well was scraped after the addition of 1.25 mL ice-cold PBS. The mixture was centrifuged at 500*g* for 10 min at 4 °C and the supernatant was again aspirated. The remaining pellet was solubilized in lysis buffer supplemented with 1% protease inhibitor and thoroughly mixed. This mixture was further sonicated on ice for 4 min, and the lysate was centrifuged at 7500*g* for 10 min at 4 °C to remove the debris present. The supernatant, which contained the proteins of interest, was diluted and aliquoted for protein determination by the Lowry's method [38]. Proximal kidney cells (Invitro ADMET, Columbia, MD) were processed in identical fashion; pieces of human liver tissue (Invitro ADMET) were homogenized in buffer containing 250 mM sucrose, 10 mM HEPES, and 10 mM Trizma base, pH 7.4. The lysate, the proximal cell, liver tissue homogenate, and human adult normal kidney tissue homogenate (BioChain Institute, Newark, CA, Catalog #P1234142; 100 µg; kind gift of Dr. Rommel G. Tirona, University of Western Ontario, London, ON) were separated by 7.5–12% SDS-polyacrylamide electrophoresis and transferred onto nitrocellulose membranes (Amersham GE Healthcare Biosciences, Pittsburgh, PA), then blocked in 5% skim milk dissolved 0.1% Tween-20 (TBS-T, Sigma-Aldrich, St. Louis, MO) in Tris-buffered saline, pH 7.4 for 1 h at room temperature, followed by incubation with the primary antibody solution (1:15000 v/v for GAPDH and 1:1000 v/v for other CYP2R1, CYP27B1, and CYP24A1 antibodies) in 2% skim milk in 0.1% TBS-T overnight at 4 °C. On the following day, membranes were washed and further incubated at room temperature for 2 h in the anti-rabbit or anti-goat secondary antibody solution (1:10000 v/v anti-mouse for GAPDH, 1:1000 v/v secondary for the other antibodies), washed three times with 0.1% TBS-T, imaged using enhanced chemiluminescence (ECL) reagents (Amersham GE Healthcare Biosciences, Pittsburgh, PA), and quantified by densitometry. Protein expression levels of CYP2R1, CYP27B1 and CYP24A1 were normalized to that of GAPDH.

2.5. Statistical analysis

Data are represented as mean ± SD. Differences between treatment groups for all cell types were evaluated using Student's two-tailed *t*-test, and a *P*-value of < 0.05 vs. vehicle control (0.1% ethanol) was viewed as statistically significant.

3. Results

3.1. Application of in vitro screens to vitamin D precursors: $1\alpha(OH)D_3$ and $25(OH)D_3$, and $1,25(OH)_2D_3$

3.1.1 Activities of vitamin D precursors: luciferase screens towards $25(OH)D_3$ and $1\alpha(OH)D_3$, with or without KTZ

When the luciferase gene reporter assay was utilized to determine the potencies (EC_{50}s) of the precursors, both $25(OH)D_3$ and $1\alpha(OH)D_3$ were found to induce luciferase activation with similar EC_{50}s of 272 and 257 nM, respectively. Upon co-incubation of the HEK293 cells with 10 µM KTZ (found to be nontoxic among all preliminary experiments), the luciferase activity following $25(OH)D_3$ treatment was significantly blunted, and a lower apparent E_{max} (expressed as RLUs) but higher EC_{50} of 608 nM compared to those in the absence of KTZ (Fig. 1). For $1\alpha(OH)D_3$, the apparent E_{max} (RLUs) was reduced following KTZ co-incubation (−KTZ/+KTZ ratio of > 272/43 or 6.3-fold for $25(OH)D_3$ and > 294/116 or 2.5-fold for $1\alpha(OH)D_3$); but there was a decrease in the apparent EC_{50} (from 257 to 147 nM). By contrast, the apparent EC_{50}s and E_{max}s (RLUs) of $1,25(OH)_2D_3$ remained relatively unchanged, with or without KTZ.

3.1.2 Changes in activities of 100 nM $25(OH)D_3$, $1\alpha(OH)D_3$ and $1,25(OH)_2D_3$ with 10 µM KTZ in HEK293 cells

The induction of CYP24A1, CYP3A4 and MDR1 mRNA expression by $1,25(OH)_2D_3$ was the highest, and KTZ inhibition failed to alter the pattern of induction. In contrast, there was little change in the mRNA levels of CYP24A1, CYP3A4, and MDR1 with $25(OH)D_3$, with or without KTZ. Compared with $1,25(OH)_2D_3$, $1\alpha(OH)D_3$ was less active, and this synthetic analog resulted in increased mRNA expression of CYP24A1 (3.9 vs. 292-fold), CYP3A4 (3.2 vs.1.6-fold) and MDR1 (1.3 vs. 1.4-fold) relative to the control (0.1% ethanol) when KTZ was absent (white bar, Fig. 2A), showing that CYP24A1 and CYP3A4

Table 1
Human primer sequences for qPCR.

	Gene Bank Number	Forward Sequence (5′ → 3′)	Reverse Sequence (5′ → 3′)
CYP24A1	NM_000782.4	CAGCGAACTGAACAAATGGTCG	TCTCTTCTCATACAACACGAGGCAG
CYP3A4	NM_017460.5	CATTCCTCATCCCAATTCTTGAAGT	CCACTCGGTGCTTTTGTGTATCT
GAPDH	NM_002046.4	GAAGGTGAAGGTCGGAGTC	GAAGATGGTGATGGGATTTC
MDR1	NM_000927	TGCTCAGACAGGATGTGAGTTG	AATTACAGCAAGCCTGGAACC
OATP1A2	NM_021094.3	TGGGGAACTTTGAAATGTGG	AAGGCTGGAACAAAGCTTGA
TRPV6	NM_018646.4	GGTTCCTGCGGGTGGAA	CCTGTGCGTAGCGTTGGAT

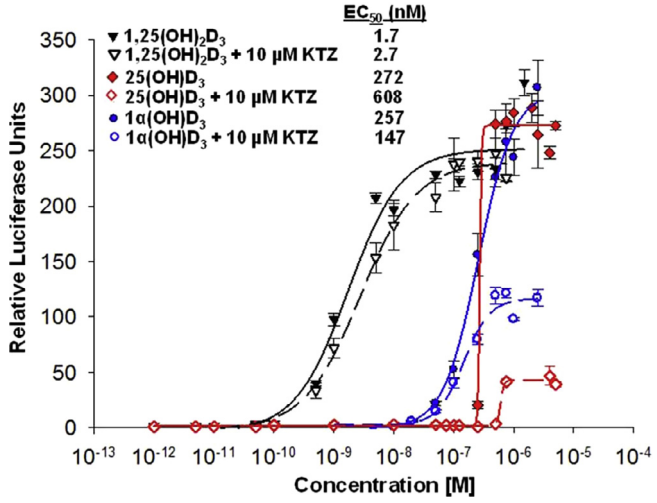

Fig. 1. Vitamin D analogs are less potent than $1,25(OH)_2D_3$ at activating VDR, and the response is blunted by 10 μM ketoconazole (KTZ) in HEK293 cells. HEK293 cells were transfected with the GAL4-hVDR, in the absence and presence of KTZ and varying concentrations of $1,25(OH)_2D_3$, $25(OH)D_3$, and $1\alpha(OH)D_3$ and were assayed for luciferase activity. Transcriptional activities in the absence of KTZ (solid lines) are $1,25(OH)_2D_3 \gg 25(OH)D_3 \approx 1\alpha(OH)D_3$. In the presence of KTZ (dashed lines), luciferase activity in HEK293 cells following $25(OH)D_3$ treatment was significantly blunted (apparent EC_{50} increased from 272 to 608 nM), and that after $1\alpha(OH)D_3$ treatment was decreased from 257 to 147 nM, while apparent EC_{50} following KTZ co-treatment with $1,25(OH)_2D_3$ remained unchanged. Results are in normalized luciferase units (RLUs) and are mean ± SD of three experiments, with sampling performed in triplicate.

induction was reduced upon addition of KTZ (black bar, Fig. 2A). These data suggest that KTZ reduced the VDR-mediated activation of $1\alpha(OH)D_3$ but not of $1,25(OH)_2D_3$ (Fig. 2A).

3.1.3 VDR target genes and formation of $1,25(OH)_2D_3$ from $25(OH)D_3$ and $1\alpha(OH)D_3$, in presence or absence of 10 μM KTZ, in HEK293 cells

The discrepancies seen between the luciferase assays in HEK293 cells and induction levels following treatment with the vitamin D precursors and KTZ (Fig. 1) are likely due to differences in the endogenous vitamin D bioactivation or degradation enzymes. We first determined whether VDR targets such as CYP24A1, CYP3A4, and MDR1 mRNA and biotransformation of $25(OH)D_3$ and $1\alpha(OH)D_3$ to $1,25(OH)_2D_3$ were altered in HEK293 cells in the presence of 10 μM KTZ. In absence of KTZ, a ranking was readily established for CYP24A1, CYP3A4, and MDR1 mRNA expressions, with $1,25(OH)_2D_3 > 1\alpha(OH)D_3 > 25(OH)D_3$; a blunting of induction was achieved upon the addition of KTZ (Fig. 2A). Notably, $1,25(OH)_2D_3$ was detected from $25(OH)D_3$ and $1\alpha(OH)D_3$ in the total incubation mixture by EIA after 16 h of incubation, with more conversion from $1\alpha(OH)D_3$ than $25(OH)D_3$ (Fig. 2B). The observed % conversion was < 0.1% for $25(OH)D_3$ and < 0.25% for $1\alpha(OH)D_3$, and addition of KTZ diminished the conversion of both precursors to $1,25(OH)_2D_3$ (Fig. 2C).

3.1.4. Basal, relative mRNA and protein expression of enzymes in HEK293 cells as well as hCMEC/D3 and Caco-2 cells

We further compared the mRNA expression levels of CYP27B1 (for $25(OH)D_3$ bioactivation), CYP2R1 (for $1\alpha(OH)D_3$ bioactivation) and CYP24A1 (for degradation of $1,25(OH)_2D_3$ and $25(OH)D_3$) (Fig. 3). The mRNA expression levels of CYP2R1 were present abundantly in Caco-2 > HEK293 ≫ hCMEC/D3 cells. For CYP27B1, the mRNA expressions were similar for HEK293 and Caco-2 cells and lesser for hCMEC/D3 cells. For CYP24A1, mRNA levels were within 2-fold difference for all cell types (Fig. 3C). The basal protein expression levels, were however, different from the mRNA expression levels (compare Fig. 3A–C vs. D–F). CYP2R1 and CYP27B1 protein levels were highest in HEK293 cells, and levels for Caco-2 and hCMEC/D3 cells were considerably lower (20–25%). By contrast, levels of CYP24A1 protein expression were comparable among all the cell types (Fig. 3F). The relatively lower CYP2R1 and CYP27B1 protein levels in the Caco-2 and hCMEC/D3 cells suggest a lesser extent of bioactivation following $25(OH)D_3$ or $1\alpha(OH)D_3$ treatment and consequently, a lower induction of VDR target genes. Generally speaking, KTZ treatment did not alter the protein levels, but was expected to exert inhibition on the activities of the enzymes.

3.1.5 $1,25(OH)_2D_3$ formation from precursors, $25(OH)D_3$ and $1\alpha(OH)D_3$, in HEK293 cells contributed to VDR activity

In view of the presence of bioactivation enzymes in forming $1,25(OH)_2D_3$ (Fig. 2B and 2C) via CYP27B1 (for $25(OH)D_3$) and CYP2R1 (for $1\alpha(OH)D_3$) (Fig. 3), we searched for the mechanisms underlying the changes in EC_{50} (0.6 to 2.2-fold) and E_{max} (2.5 to 6.3 fold) for $25(OH)D_3$ and $1\alpha(OH)D_3$ in the absence and presence of KTZ. When the interaction between $25(OH)D_3$ or $1\alpha(OH)D_3$ (0.1 to 500 nM) and $1,25(OH)_2D_3$ in the presence of 10 μM KTZ was examined in the GAL4-hVDR transfection system, a lack of change in the RLUs of 10 nM $1,25(OH)_2D_3$ was observed in the presence of KTZ (Fig. 4). The lack of interaction between $1,25(OH)_2D_3$ and $25(OH)D_3$ or $1\alpha(OH)D_3$ provided the basis of our simulations. We made an assumption that the concentration of $25(OH)D_3$, $1\alpha(OH)D_3$, or $1,25(OH)_2D_3$ in the incubation medium and HEK293 cells behaved as one homogeneous compartment. The likelihood is high since the vitamin D analogs are lipophilic substrates of high log*P* values (> 5), and the concentration of $1,25(OH)_2D_3$ in the incubation medium was found similar to that in the total incubation system (cell + medium) (unpublished data), with $1,25(OH)_2D_3$ equilibrating quickly among tissues in the mouse (35). We estimated the conversion of $25(OH)D_3$ to $1,25(OH)_2D_3$ using the literature K_m value of 2.7 μM (for mouse and man) (15). Since the V_{max} for formation is unknown in HEK293 cells, we adjusted the $V_{max}^{25(OH)D_3 \rightarrow 1,25(OH)_2D_3}$ value in Eq. (1) by trial and error to optimize the residual sum of squares, and arrived at 22,500 arbitrary units per unit volume (see Table 2). Based on these constants, the simulations obtained matched the observations on the $25(OH)D_3$ concentration-activity profiles, in absence and presence of KTZ (Fig. 5A), with curvatures that are similar to those observed in Fig. 1.

$$C_{1,25(OH)_2D_3\ formed} = \frac{V_{max}^{25(OH)D_3 \rightarrow 1,25(OH)_2D_3} C_{25(OH)D_3}}{K_m^{25(OH)D_3 \rightarrow 1,25(OH)_2D_3} + C_{25(OH)D_3}} \quad (1)$$

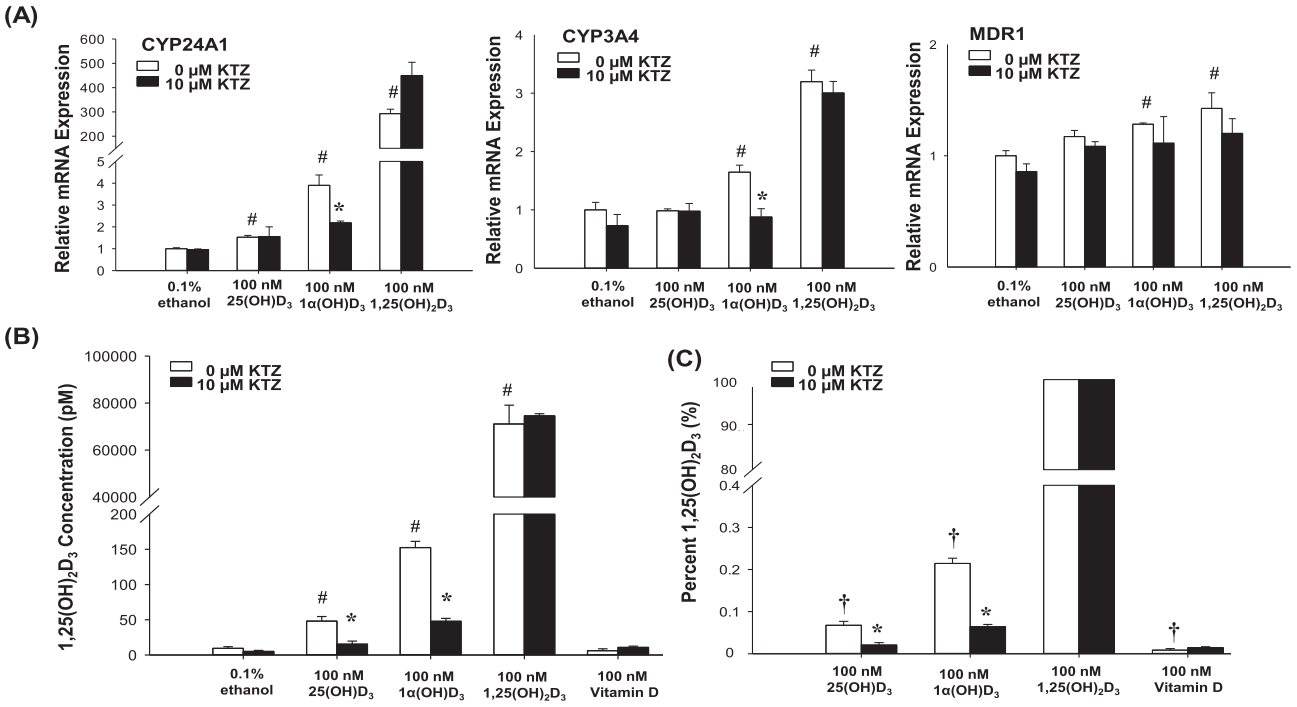

Fig. 2. Relative mRNA expression of VDR-target genes (A), and levels of the active metabolite, $1,25(OH)_2D_3$ (B, C), in lysates of HEK293 cells treated with 100 nM $25(OH)D_3$, $1\alpha(OH)D_3$, and $1,25(OH)_2D_3$ ± 10 μM ketoconazole (KTZ); vitamin D_3 was used as a negative control. In absence of KTZ (white bars), $1\alpha(OH)D_3$ significantly increased the mRNA expression of VDR-target genes (CYP24A1, CYP3A4, and MDR1); mRNA levels were lower than those after incubation with $1,25(OH)_2D_3$ but greater than those of $25(OH)D_3$. Induction of CYP24A1/CYP3A4 mRNA expression by $1\alpha(OH)D_3$ was reduced after addition of KTZ (black bars); there was little change in the extent of induction of CYP24A1, CYP3A4, and MDR1 for $25(OH)D_3$ and $1,25(OH)_2D_3$, with or without KTZ. The pattern of KTZ inhibition was similar to the concentration of $1,25(OH)_2D_3$ formed (B) or the proportion (normalized to $1,25(OH)_2D_3$ in HEK293, as 100%) of $1,25(OH)_2D_3$ (C). Data are mean ± SD of three experiments with sampling performed in triplicate; # denotes $P < 0.05$ for $25(OH)D_3$– or $1\alpha(OH)D_3$– or $1,25(OH)_2D_3$–treated vs. 0.1% ethanol (control) with 0 μM KTZ; * denotes $P < 0.05$ vs. 0 μM KTZ in respective treatment groups; † denotes $P < 0.05$ for $25(OH)D_3$- or $1\alpha(OH)D_3$-treated vs. $1,25(OH)_2D_3$–treated HEK293 cells; vitamin D_3 was added as a negative control to quantify the extent of conversion to $1,25(OH)_2D_3$.

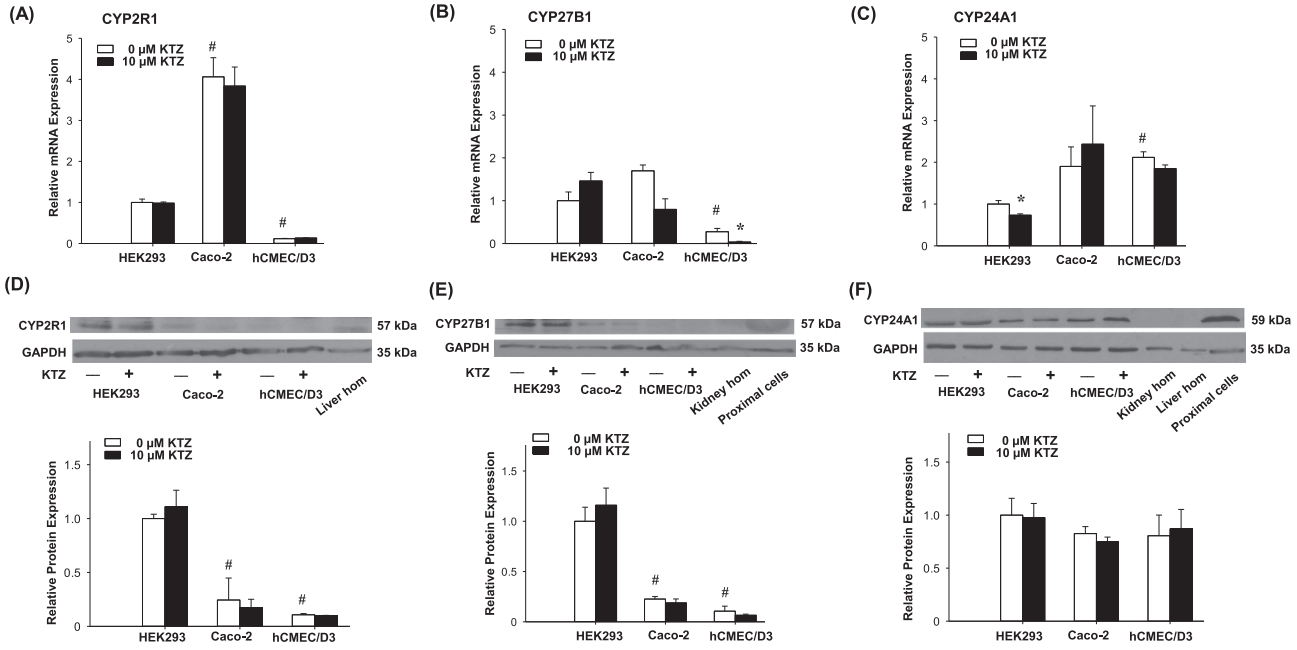

Fig.3. Relative basal mRNA (A to C) and protein (D to F) expression of enzymes CYP2R1, CYP27B1 and CYP24A1 in HEK293, Caco-2 and hCMEC/D3 cells normalized to GAPDH, against whole kidney homogenate (kidney hom), and renal proximal cell and liver homogenates (liver hom) as standards. Cells were co-incubated with vehicle (0.1% ethanol or 0.1% ethanol and 10 μM KTZ) for HEK293 (1 day) and hCMEC/D3 or Caco-2 cells (3 days). A comparable relative protein expression pattern was observed for CYP24A1 in HEK293, Caco-2 and hCMEC/D3 cells, whereas the relative protein expression levels of CYP2R1 and CYP27B1 were significantly lower in Caco-2 and hCMEC/D3 cells compared with HEK293 cells. Data are mean ± SD of three experiments with sampling performed in triplicate. * denotes $P < 0.05$ for Caco-2 and hCMEC/D3 vs. HEK293 cells.

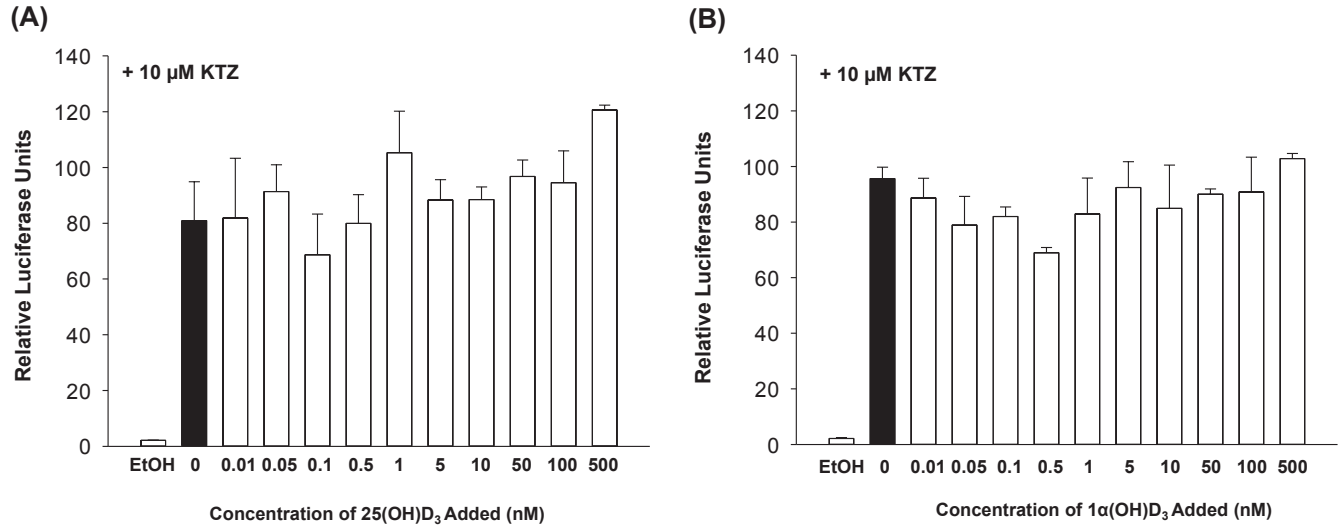

Fig. 4. Lack of effect of 25(OH)D_3 (A) or 1α(OH)D_3 (B) on the potency of 1,25$(OH)_2D_3$. Co-incubation of 0.1 to 500 nM 25(OH)D_3 (A) or 1α(OH)D_3 (B) with 10 nM 1,25$(OH)_2D_3$ did not affect the luciferase activity of 10 nM 1,25$(OH)_2D_3$ in the GAL4-hVDR assay, showing that 25(OH)D_3 and 1α(OH)D_3 are not partial agonists. Data are mean ± SD with sampling performed in triplicate.

Table 2
Literature parameters on K_m values for 1,25$(OH)_2D_3$ formation from the precursors, and the observed EC_{50}s and E_{max}s (obtained from fit by Prism for data in Fig. 1) were used to predict individual activities of 25(OH)D_3 or 1α(OH)D_3 with that of the active metabolite 1,25$(OH)_2D_3$ formed.

RLU Data Sets	Luciferase Assay		Formation of 1,25$(OH)_2D_3$	
	EC_{50} (pM)	E_{max} (RLU)	K_m (pM)	V_{max}[a] (arbitrary units per unit volume)
25(OH)D_3 (+KTZ)	608,000	48	2,700,000[b]	22,500
1α(OH)D_3 (+KTZ)	147,000	116	9,600,000[c]	41,000
1,25$(OH)_2D_3$[d] (± KTZ)	2,200 (average of 1.7 and 2.7 nM)	245 (average of 251 and 239 RLUs)		

[a] Obtained by trial and error towards lowest weighted residual sum of squares.
[b] Assigned, according to (15).
[c] Assigned, according to (23).
[d] Parameter values (± KTZ) were averaged since there was no major difference, with or without KTZ.

We did not consider the Hill coefficient, γ, which may appear as the exponent to the concentration terms; here we assume that γ is one.

The corresponding RLU was given by the E_{max}s (RLU) and EC_{50}s of preformed 1,25$(OH)_2D_3$ (245 RLU and 2.2 nM, respectively; see Table 2 for these averaged values) described in Eq. (2).

$$RLU_{1,25(OH)_2D_3 formed} = \frac{E_{max}^{1,25(OH)_2D_3} C_{1,25(OH)_2D_3 formed}}{EC_{50}^{1,25(OH)_2D_3} + C_{1,25(OH)_2D_3 formed}} \quad (2)$$

The RLU associated with 25(OH)D_3 alone was revealed by the data of 25(OH)D_3 in the presence of KTZ, with the E_{max} of about 43 RLU and EC_{50} of 608 nM. The total RLU for 25(OH)D_3 in the absence of KTZ was given by summing of the RLU of the metabolite (Eq. (2) to the RLU for 25(OH)D_3 when KTZ is present:

$$RLU_{25(OH)D_3\ total}^{-KTZ} = RLU_{1,25(OH)_2D_3\ formed}^{-KTZ} + RLU_{25(OH)D_3}^{+KTZ}$$
$$= \frac{E_{max}^{1,25(OH)_2D_3} C_{1,25(OH)_2D_3 formed}}{EC_{50}^{1,25(OH)_2D_3} + C_{1,25(OH)_2D_3 formed}} + \frac{E_{max}^{25(OH)D_3 + KTZ} C_{25(OH)D_3}}{EC_{50}^{25(OH)D_3 + KTZ} + C_{25(OH)D_3}} \quad (3)$$

The total conversion of 25(OH)D_3 to 1,25$(OH)_2D_3$ was estimated to be < 0.83% [0.83% to 0.18% for 25(OH)D_3 concentrations ranging from 1 to 10,000,000 pM], with a predicted RLU ratio for 25(OH)D_3 (−KTZ/+KTZ) of 6.37 (Fig. 5A), although the highest RLU (−KTZ) value has not been reached for the E_{max} (−KTZ).

When the same strategy was used to predict the curves for 1α(OH)D_3, by utilizing similar equations for the conversion of 1α(OH)D_3 to 1,25$(OH)_2D_3$ and assigning the literature K_m value of 9.6 μM (23), an optimized $V_{max}^{1\alpha(OH)D_3 \rightarrow 1,25(OH)_2D_3}$ value of 41,000 arbitrary unit was obtained (Table 2). The conversion of 1α(OH)D_3 to 1,25$(OH)_2D_3$ was estimated to be 0.42% [0.42% to 0.21% for 1α(OH)D_3 concentrations ranging from 1 to 10,000,000 pM]; the predicted RLU ratio (−KTZ/+KTZ) ratio was of 2.94; again, the highest RLU (−KTZ) value has not been reached for the E_{max}. The RLU of the formed, active metabolite (Eq. (2) was then added to the RLU expected for intact 1α(OH)D_3 (+KTZ), based on a EC_{50} of 147 nM and E_{max} of 116 RLU (see Table 2). Profiles exceedingly similar to those observed were again obtained (Fig. 5B). For both precursors, we were unable to predict nor explain the steep and abrupt rise observed among the curves.

3.1.6. Activities of 25(OH)D_3, 1α(OH)D_3 and 1,25$(OH)_2D_3$ and KTZ in hCMEC/D3 cells

When hCMEC/D3 cells were used to appraise the extent of induction, it was expected that the bioactivation product, 1,25$(OH)_2D_3$, would induce CYP24A1 expression levels. The mRNA expression levels of CYP24A1 were found to be dramatically elevated over the 0.1% ethanol control for 25(OH)D_3 treatment, and levels were even higher for 1α(OH)D_3 and 1,25$(OH)_2D_3$. For 1α(OH)D_3 and 25(OH)D_3, the CYP24A1 mRNA expression levels returned back to vehicle control levels when KTZ was added to the system (Fig. 6A). For 1,25$(OH)_2D_3$, there was a small but significant reduction of CYP24A1 expression levels with KTZ; the reason is, however, unknown. Both MDR1 mRNA (Fig. 6B) and P-gp protein (Fig. 6C) expression levels were increased significantly for 1α(OH)D_3 and 1,25$(OH)_2D_3$ but not for 25(OH)D_3.

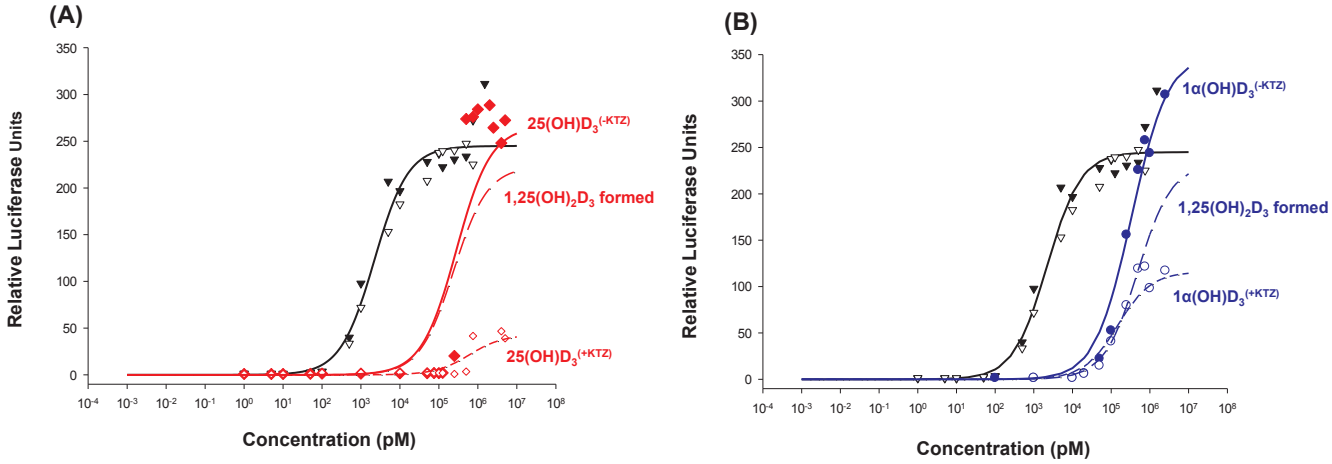

Fig. 5. Simulated data (lines) based on parameters shown in Table 2 vs. observed (symbols) luciferase activities of $1,25(OH)_2D_3$ and the precursors ± KTZ. The observed luciferase activity of preformed $1,25(OH)_2D_3$, in absence (▼) and presence (∇) of KTZ were presented against the simulations (black line), and (A) $25(OH)D_3^{(-KTZ)}$ (♦) and $25(OH)D_3^{(+KTZ)}$ (◊) vs. the predicted luciferase activity of $25(OH)D_3$ (± KTZ) and formed $1,25(OH)_2D_3^{(-KTZ)}$ (red lines); (B) $1\alpha(OH)D_3^{(-KTZ)}$ (●) and $1\alpha(OH)D_3^{(+KTZ)}$ (○) data vs. the predicted RLUs of $1\alpha(OH)D_3$ (± KTZ) and formed $1,25(OH)_2D_3^{(-KTZ)}$ (blue lines). See text for details. (For interpretation of the references to color in this figure legend, the reader is referred to the web version of this article.)

3.1.7 Activities of 25(OH)D₃, 1α(OH)D₃ and 1,25(OH)₂D₃ and KTZ in Caco-2 cells

Incubation of Caco-2 cells with 100 nM $1,25(OH)_2D_3$ over the last 3 days of the 21-day culture period led to an increase in the mRNA expression of VDR-target genes: CYP24A1 (3,200-fold), CYP3A4 (180-fold), TRPV6 (245-fold), and OATP1A2 (12-fold), when compared to those incubated with 0.1% ethanol (control) (Fig. 7). The extent of induction with 100 nM $1\alpha(OH)D_3$ was comparable to, though less than that of $1,25(OH)_2D_3$, whereas induction was low with $25(OH)D_3$. Co-incubation of 10 KTZ with $1,25(OH)_2D_3$ reduced the mRNA expression of CYP3A4 (86%), TRPV6 (62%), and OATP1A2 (32%), but increased the mRNA expression of CYP24A1 (1.6-fold); the latter levels rose because of inhibition of CYP24A1 by KTZ, rendering higher induction by $1,25(OH)_2D_3$ on CYP24A1. KTZ co-treatment with $1\alpha(OH)D_3$ also significantly reduced the extent of induction; the mRNA expression of CYP24A1, CYP3A4, TRPV6, and OATP1A2 fell to 73%, 99%, 93% and 69%, respectively, relative to levels elevated in the absence of KTZ. Comparatively speaking, $1,25(OH)_2D_3$ activities were lower with KTZ, but the extent of decrease (32–86%) was less than that (69–99%) observed with $1\alpha(OH)D_3$. This change was unexpected since the 10 μM concentration KTZ was pre-determined to be non-toxic (data not shown). The mRNA expression of the VDR-target genes following $25(OH)D_3$ treatment remained low and unchanged, when KTZ was absent or present, and levels were basically similar to that of vehicle control (Fig. 7).

3.2. Application of in vitro screens to Teijin compounds

3.2.1 Characterization of Teijin compounds for VDR activity in HEK293 cells

$1,25(OH)_2D_3$, the endogenous ligand, was a potent compound (EC_{50} 1.7 to 2.7 or average of 2.2 nM), and the parameters were unaffected by KTZ treatment, whereas the Teijin compounds were found to activate the hVDR at varying degrees (Fig. 8). Compared to observations in absence of KTZ, all Teijin compounds were able to interact with hVDR, with generally unchanged E_{max} values when KTZ was present (TPD-004, TPD-006, TPD-007, TPD-008, TPD-009, TPD-010, and TPD-011), although for others (TPD-001, TPD-002, TPD-003, and TPD-005), the

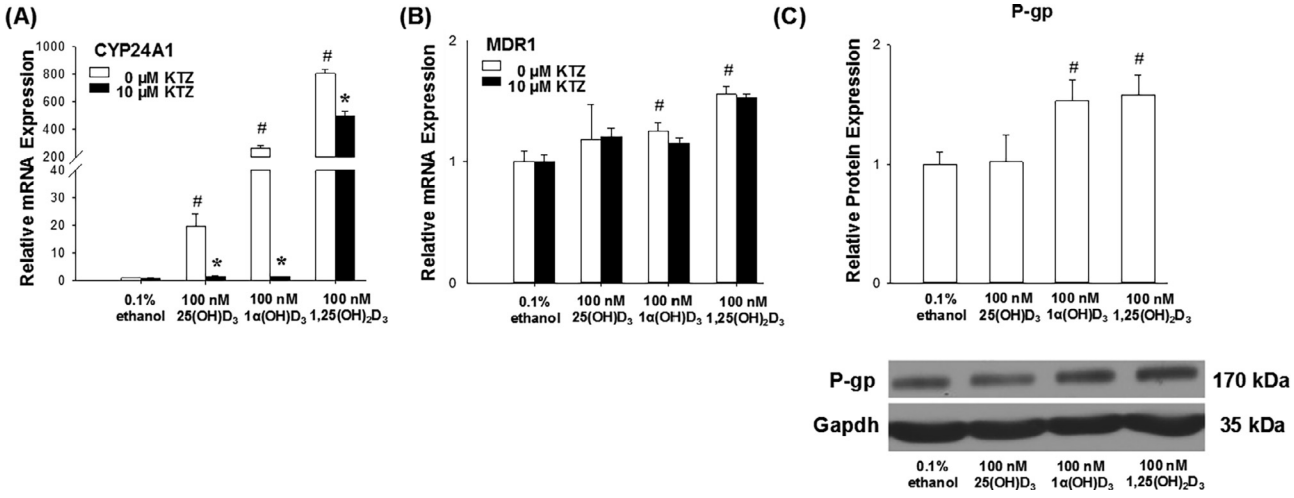

Fig. 6. Relative mRNA expression of CYP24A1 (A) and MDR1 (B) in hCMEC/D3 cells treated with 100 nM $25(OH)D_3$, $1\alpha(OH)D_3$, and $1,25(OH)_2D_3$ ± 10 μM ketoconazole (KTZ) and P-gp protein expression levels (C) in hCMEC/D3 cells. Treatment with $1\alpha(OH)D_3$ and $1,25(OH)_2D_3$ significantly induced MDR1 mRNA and P-gp protein expression levels. The induction of CYP24A1 but not MDR1 was significantly blunted by KTZ for $1\alpha(OH)D_3$ and $1,25(OH)_2D_3$. Data are mean ± SD of 3 experiments, with sampling performed in triplicate; # denotes $P < 0.05$ for $1\alpha(OH)D_3$- or $1,25(OH)_2D_3$-treated vs. 0.1% ethanol (control) with 0 μM KTZ; * denotes $P < 0.05$ for 0 vs. 10 μM KTZ in respective treatment groups.

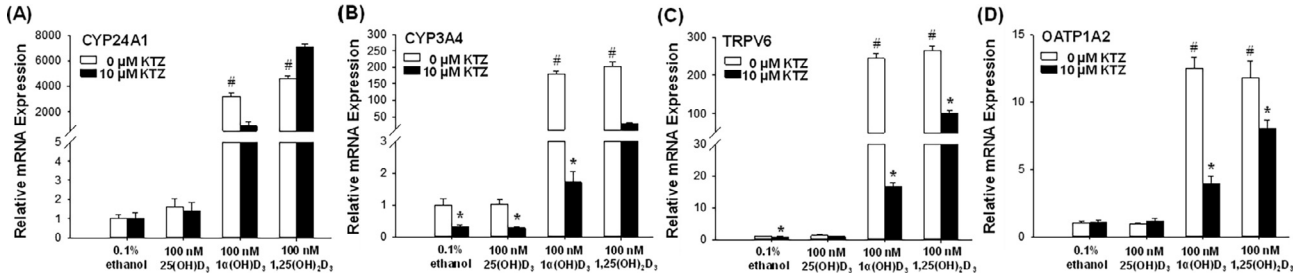

Fig. 7. Relative mRNA expression of VDR-target genes in Caco-2 cells treated with 100 nM $25(OH)D_3$, $1\alpha(OH)D_3$, and $1,25(OH)_2D_3$ ± 10 μM ketoconazole (KTZ). Treatment of Caco-2 cells with $1\alpha(OH)D_3$ significantly increased the mRNA expression levels of CYP24A1, CYP3A4, TRPV6, and OATP1A2 to levels similar to those of $1,25(OH)_2D_3$. The level of induction observed for $1\alpha(OH)D_3$ was significantly inhibited by KTZ. In contrast, $25(OH)D_3$ treatment showed no induction of VDR target genes. Data are mean ± SD of three experiments with sampling performed in triplicate; # denotes $P < 0.05$ for $1\alpha(OH)D_3$- or $1,25(OH)_2D_3$-treated vs. 0.1% ethanol (control) with 0 μM KTZ; * denotes $P < 0.05$ for 0 vs. 10 μM KTZ in respective treatment groups.

E_{max} values were reduced, suggesting metabolic removal and/or inactivation (see values and ratios, Table 3, Fig. 8). Among these, TPD-003, TPD-005, TPD-006, TPD-008 and TPD-009 displayed superagonist potencies, with EC_{50}'s < 1 nM. Others – TPD-001, TPD-007, TPD-013 and TPD-090 – displayed excellent potencies (between 1 and 10 nM), and TPD-002 (67 nM), moderate potency. The EC_{50} values for TPD-012 (2732 nM, in the absence of KTZ) and TPD-014 (1526 nM, in the presence of KTZ) were much higher, and may be partial agonists (Table 3).

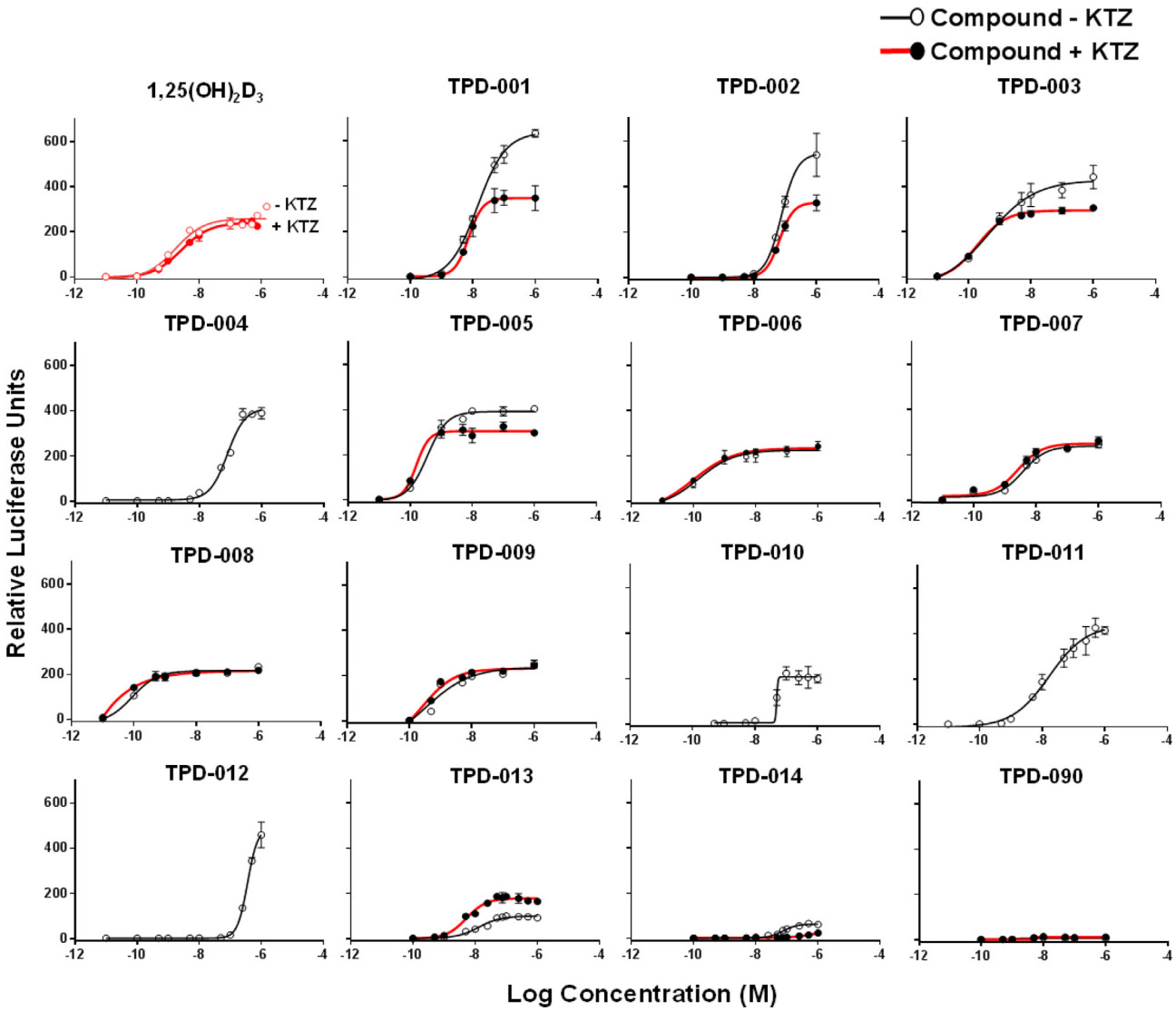

Fig. 8. Dose-response curves of Teijin compounds ± ketoconazole (10 μM KTZ) in HEK293 cells demonstrating VDR agonistic activity. HEK293 cells were co-transfected with GAL4-hVDR and UAS-luciferase reporter and 6–8 h after were treated with 0.1% ethanol (negative control) ± KTZ or with increasing concentrations of the Teijin compounds ± 10 μM KTZ or $1,25(OH)_2D_3$ (positive control) ± KTZ. Cells were assayed for luciferase activity 16 h later. Data are mean ± SD (n = 3). Relative luciferase units = (luciferase light units/β-galactosidase) * time. The response from the negative control was set to 1.

Table 3
Structures of Teijin compounds, apparent EC_{50}s, E_{max}s, and ratios ± KTZ from hVDR-transfected HEK293 cells.

Teijin Compound	Structure	EC_{50+KTZ} (nM)	EC_{50-KTZ} (nM)	$\frac{EC_{50+KTZ}}{EC_{50-KTZ}}$	$E_{max+KTZ}$ (RLU)[a]	$E_{max-KTZ}$ (RLU)[a]	$\frac{E_{max+KTZ}}{E_{max-KTZ}}$
TPD-001	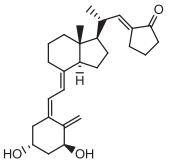	7.5	15	0.5	347	632	0.55
TPD-002	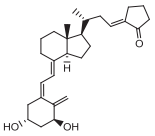	67	77	0.87	329	540	0.61
TPD-003	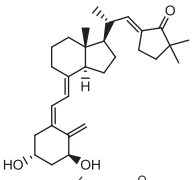	0.17	0.3	0.57	305	442	0.69
TPD-004	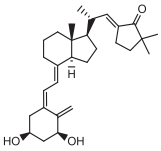	–[b]	70	–[b]	–[b]	390	–[b]
TPD-005	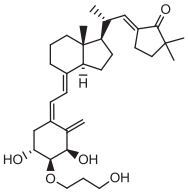	0.14	0.25	0.56	298	403	0.74
TPD-006	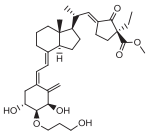	0.15	0.15	1	240	243	1
TPD-007	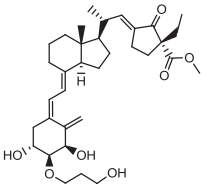	2	3	0.33	263	247	1
TPD-008	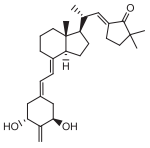	0.06	0.1	0.6	218	233	1
TPD-009	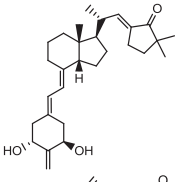	0.58	0.72	0.81	244	251	1
TPD-010	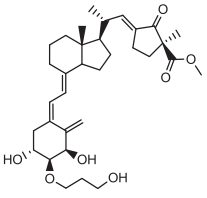	–	50	–	–	222	–

(*continued on next page*)

Table 3 (*continued*)

Teijin Compound	Structure	EC_{50+KTZ} (nM)	EC_{50-KTZ} (nM)	$\frac{EC_{50+KTZ}}{EC_{50-KTZ}}$	$E_{max+KTZ}$ (RLU)[a]	$E_{max-KTZ}$ (RLU)[a]	$\frac{E_{max+KTZ}}{E_{max-KTZ}}$
TPD-011	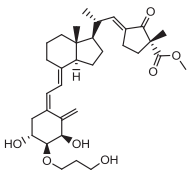	–	17	–	–	425	–
TPD-012	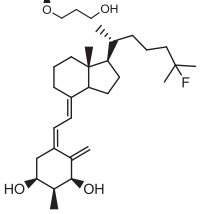	–	2730	–	–	460	–
TPD-013	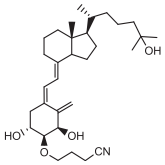	4.8	12.6	0.38	164	92	1.78
TPD-014 (TEI-9647)	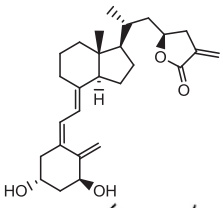	1526	75	20.3	24	61	0.39
TPD-090	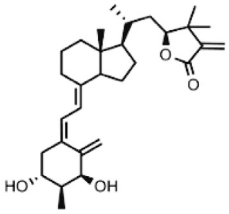	1.3	4.7	0.28	8	12	0.67
$1,25(OH)_2D_3$	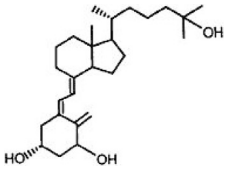	2.7	1.7	1.59	241	259	1

[a] Relative luciferase units, normalized to ethanol control.
[b] Data not available.

The potencies (EC_{50}s) of TPD-006, TPD-007, TPD-008, and TPD-009 were not affected by KTZ; but the EC_{50}s were reduced for TPD-001, TPD-002, TPD-003, TPD-005, and TPD-013 in the presence of KTZ. The ratio of the EC_{50}s in presence/absence of KTZ varied between 0.2 and 2. For TPD-014, its EC_{50} was dramatically increased in the presence of KTZ; the ratio of EC_{50}s in presence/absence of KTZ exceeded 20 (Table 3). An unusual trend was further observed for TPD-013, which showed a higher E_{max} and lower EC_{50} value when cells were treated with KTZ. The reason is unknown but may be related to degradation of the TPD-013 compound to a less active metabolite.

3.2.2 Specificity of the Teijin compounds towards activating human VDR

To assess whether the agonist properties of Teijin compounds were VDR specific, a panel of nuclear receptors (LXRα/β, FXR, GR, MR, PPARα/β/γ, and PR) was tested using the same luciferase reporter assay. HEK293 cells were co-transfected with UAS-luciferase reporter and GAL4-CMX, GAL4-hLXRα, GAL4-hLXRβ, GAL4-hFXR, GAL4-hGR, GAL4-hMR, GAL4-hPPARα, GAL4-hPPARβ, GAL4-hPPARγ, GAL4-hPR or GAL4-hVDR. The results showed that all Teijin compounds tested were selective for hVDR with the exception of TPD-012, which activated GR and PPARβ (data not shown). Unfortunately, the xenobiotic nuclear receptors hPXR and hCAR were not included to exclude their roles in ligand activation in HEK293 cells.

3.2.3 Effects of Teijin compounds in hCMEC/D3 cells

To test whether the Teijin compounds induced VDR target genes (MDR1 and CYP24A1) to the same extent as $1,25(OH)_2D_3$ in the human brain endothelial cells, we treated hCMEC/D3 with 100 nM

$1,25(OH)_2D_3$ and the Teijin compounds for 3 days. All Teijin compounds except TPD-090 significantly (> 5 to 65-fold) induced CYP24A1 levels, as did $1,25(OH)_2D_3$ (50-fold). TPD-012 provided a low induction of CYP24A1, with TPD-014, even lower, and TPD-090, not at all (Fig. 9A). The effects of the Teijin compounds on MDR1 mRNA expression were more variable. TPD-003, TPD-004, TPD-013 and TPD-014 induced MDR1 mRNA expression whereas changes for TPD-001, TPD-002, TPD-006, TPD-007, TPD-008, TPD-009, TPD-010, TPD-011, and TPD-012 were insignificant; there was no change for TPD-090 (Fig. 9B).

3.2.4 Activities of Teijin compounds in Caco-2 cells

When the activities of the Teijin compounds were monitored in Caco-2 cells after incubation with 100 nM $1,25(OH)_2D_3$ or 100 nM Teijin compounds during the last 3 days of the 21-day culture period, there was an increase in mRNA expression of VDR-target genes: CYP24A1, CYP3A4, MDR1, OATP1A2, and TRPV6 compared to 0.1% ethanol (control) (Fig. 10). The induction patterns of CYP24A1 (Fig. 10A) and CYP3A4 (Fig. 10B) were exceedingly similar. Induction patterns for MDR1 (Fig. 10C), OATP1A2 (Fig. 10D), and TRPV6 (Fig. 10E) were also similar, although the change in MDR1 mRNA expression was of a much lower magnitude. Similar magnitudes of the induction for CYP3A4 (extremely high mRNA fold-changes (200–400) and MDR1 (50% mRNA fold-change) were also observed by Aiba et al. [39]. TRPV6 fold changes in Caco-2 cells were lowest for TPD-090, then TPD-014, TPD-002, and TPD-012, with the remaining compounds showing similar response to $1,25(OH)_2D_3$. TPD-090 was ineffective as a VDRA, since there was no induction of TRPV6, CYP24A1, OATP1A2, and MDR1 expression, and TPD-014 was a weak VDRA.

4. Discussion

In vitro screens are commonplace strategies used for the estimation of pharmacological activities in silico. A tissue-sensitive VDR agonist that has selective desirable properties with avoidance of undesirable ones, namely, high induction of P-gp for increased brain efflux of amyloid-β peptides [35], a low EC_{50} in the GAL4-hVDR assay and low intestinal induction of TRPV6 in the presence of KTZ would identify new and viable VDRA candidates. The paradigm for the GAL4-hVDR assay or other in vitro screens is predicated on the concentration of intact ligand within the cell, with the assumptions that the ligand does not endure metabolism and is able to penetrate the HEK293 cellular membrane and equilibrate with that in the incubation medium. Failure to fulfill these criteria would not reflect accurately the potency of the compound. With this mandate in mind, we set off to develop screens to identify compound potency of the VDRAs from Teijin. Like others [40,41], we first utilized the GAL4-hVDR luciferase reporter assay in HEK293 cells. The transcriptional reporter assays, developed in HEK293 [40], EBNA293 [42], or HeLa/COS-7 [43] cells, are intended to appraise the potencies with EC_{50} estimates. The Caco-2 cells, historically used to assess calcium fluxes [44–46] and VDR-mediated activation of the calcium transporter CaT1 [47], also known as the transient receptor potential vanilloid type 6, TRPV6 [48] for calcium absorption [49–51] is then used to identify whether the VDRA would strongly induce TRPV6 as well as other VDR targets. Lastly, the screen for VDR activity in hCMEC/D3 cells that contain MDR1/P-gp at the luminal membrane [52,53] is used to identify the desired, targeted VDR activity. Unfortunately, $1,25(OH)_2D_3$ induces TRPV6 and causes hypercalcemia, an unwanted and negative side effect that limits its clinical use. But it is highly noteworthy that these screens have led to the identification of non-calcemic VDRAs as agonists [40], since based on these criteria, a non-hypercalcemic non-secosteroidal VDR modifier (VDRM) with cardio-protective effects has been identified [41].

The discordance in EC_{50} values (2.2-fold higher EC_{50}) in the hVDR GAL4-assay in the presence vs. absence of KTZ for $25(OH)D_3$ prompted us to examine the presence of bioactivation enzymes. In absence of KTZ, the luciferase activity towards $25(OH)D_3$ in HEK293 cells could be attributed partially to the more potent, bioactivated metabolite, $1,25(OH)_2D_3$, formed via CYP27B1. This was confirmed by simulations, showing that the mixture of $25(OH)D_3$ and $1,25(OH)_2D_3$ would collectively contribute to the apparently higher affinity (EC_{50} of 272 nM) and E_{max} for $25(OH)D_3$ that were initially observed in absence of KTZ (Fig. 5A). The observed EC_{50} and E_{max} values for $25(OH)D_3$ in the presence of KTZ would now reflect the true EC_{50} and E_{max} estimates for $25(OH)D_3$ alone, when inhibition by KTZ is complete. Despite that the formation extent predicted for $1,25(OH)_2D_3$ is only < 1% dose due to the high K_m for formation (2.7 μM) (15), the contribution to the RLU by the formed $1,25(OH)_2D_3$ is high due to its low EC_{50}. A complete agreement on the $1,25(OH)_2D_3$ formed (0.07% dose) vs. that simulated (0.83% dose) was absent and this could be due to various reasons. The

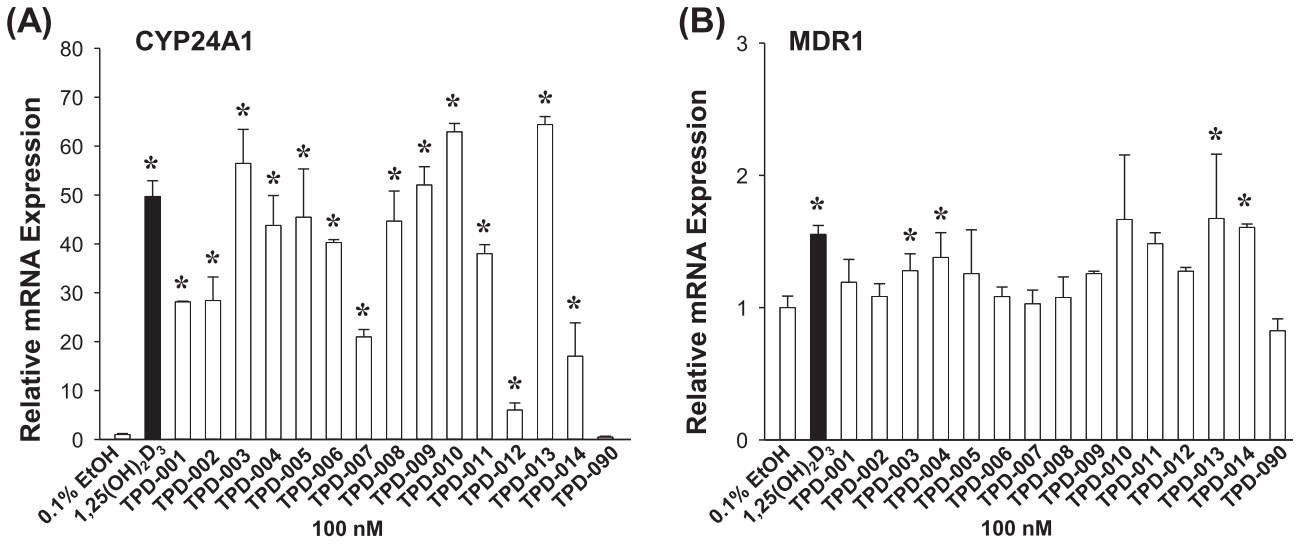

Fig. 9. Relative mRNA expression of VDR-target genes in hCMEC/D3 cells treated with 100 nM Teijin compounds or $1,25(OH)_2D_3$. Treatment of hCMEC/D3 cells with the Teijin compounds (white bars) or $1,25(OH)_2D_3$ (black bar) significantly induced the mRNA expression of the VDR-target gene CYP24A1. Brain MDR1 was only mildly induced from treatment with TPD-003, TPD-004, TPD-013 and TPD-014. Data are mean ± SD (n = 3); * denotes $P < 0.05$ vs. 0.1% ethanol (vehicle).

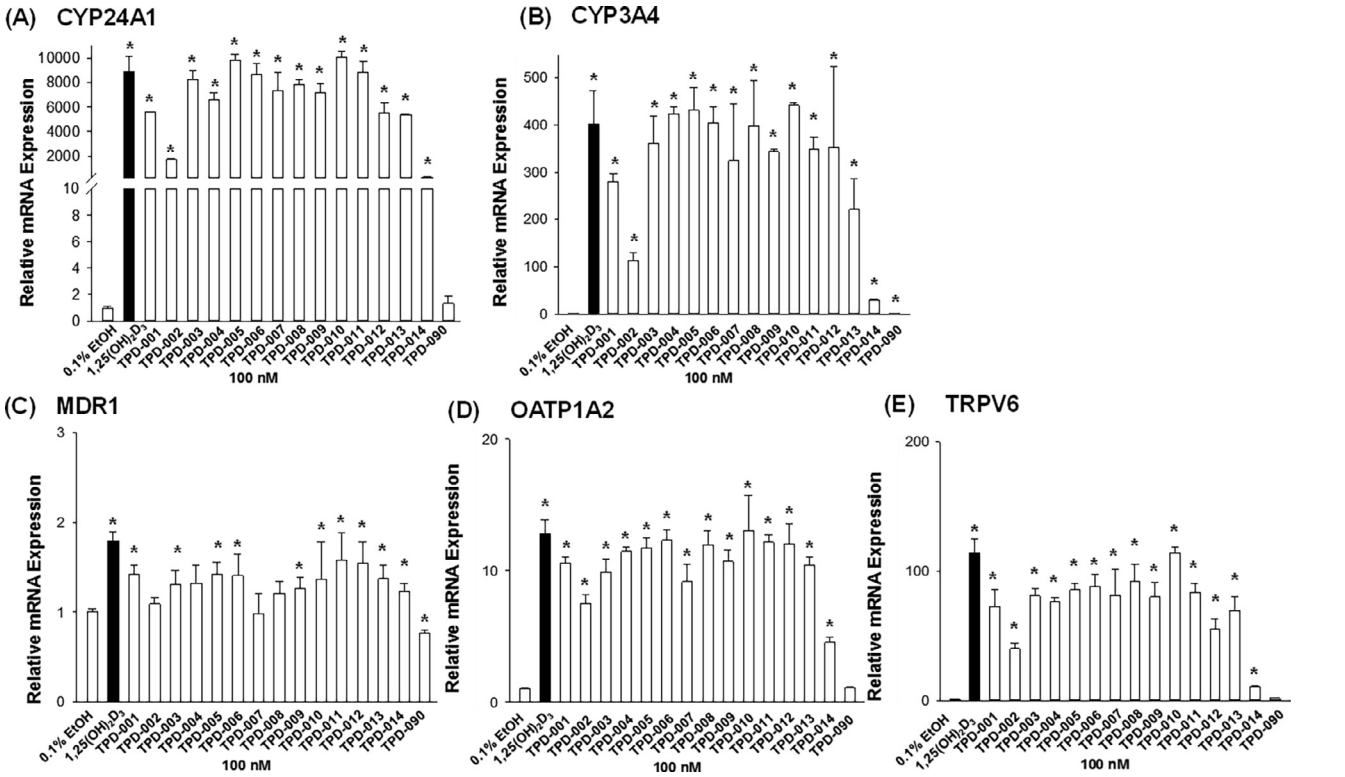

Fig. 10. Relative mRNA expression of VDR-target genes in Caco-2 cells treated with 100 nM Teijin compounds or $1,25(OH)_2D_3$. Treatment of Caco-2 cells with the Teijin compounds (white bars) or $1,25(OH)_2D_3$ (black bar) significantly induced the mRNA expression of VDR-target gene CYP24A1 (A), CYP3A4 (B), MDR1 (C), OATP1A2 (D), and TRPV6 (E). Data are mean ± SD (n = 3); * denotes $P < 0.05$ vs. 0.1% ethanol (vehicle).

$1,25(OH)_2D_3$-mediated feedback inhibition on CYP27B1 and induction of CYP3A4 and CYP24A1 (major degradation pathways of $25(OH)D_3$) [18] have not been accounted for. Moreover, $25(OH)D_3$ is a substrate of multiple enzymes: UGT1A4 and UGT1A3 (19), SULT2A1 (16, 17), CYP3A4 (20), and CYP24A1 [18]. These enzymes compete for the substrate, $25(OH)D_3$, reducing the extent of formation of $1,25(OH)_2D_3$. The sum of $25(OH)D_3$ and $1,25(OH)_2D_3$ will not constitute total mass balance. Ketoconazole will, however, inhibit not only the CYPs but also UGTs [54,55] and SULTs [56,57], and its universality as an enzyme inhibitor of both oxidative and conjugative pathways should improve the accuracy of the estimates for the cell-based systems. The same caveat exists for $1\alpha(OH)D_3$, since CYP27R1 is present for the formation of active $1,25(OH)_2D_3$, albeit at modest but detectable concentrations. Due to bioactivation to $1,25(OH)_2D_3$, the apparent EC_{50} was altered slightly, and the E_{max} value, reduced with KTZ. Simulation of the RLUs based on $1\alpha(OH)D_3$ and the active $1,25(OH)_2D_3$ formed with or without KTZ (Fig. 5B) again confirmed the bioactivation pattern.

Probing into the presence of mRNA and protein expression of enzymes among Caco-2 cells, we found lower basal protein levels of CYP2R1 (less than half) and much lower levels of CYP27B1 but similar CYP24A1 levels compared to those in HEK293 cells (Fig. 3). Since Caco-2 cells contain appreciable protein expression levels of the bioactivation enzymes, there is again the need to include KTZ for an accurate estimation of the potencies of the intact VDRAs on the VDR target genes. As expected, the effect of KTZ is greater for $1\alpha(OH)D_3$ due to the higher levels of CYP2R1 present, while the effect on $25(OH)D_3$ is lower due to the low CYP27B1 protein content (Fig. 3E). For hCMEC/D3 cells, where expression levels of the enzymes were low, we found that P-gp and MDR1 expression were increased with incubation of $1,25(OH)_2D_3$ and $1\alpha(OH)D_3$ but not $25(OH)D_3$ due to its innate, low potency (Fig. 6).

With KTZ added to these screens, we proceeded to identify suitable intact VDRAs that would induce brain MDR1 in hCMEC/D3 cells in the absence of enhanced bioactivation or degradation. Among the Teijin compounds studied, we examined the activities of three structural features: (i) the cyclopentanone (TPD-001 to TPD-011) that contain the α,β-unsaturated ketone moiety, (ii) the straight side chain (TPD-012 and TPD-013), and (iii) the lactone (TPD-014 and TPD-090) derivatives. The Teijin cyclopentanone moieties are more rigid than the straight chain derivatives, forcing the oxygen atom placement onto appropriate locations for hydrogen bonding with the His305/His397 of the VDR-ligand binding site (VDR-LBD, ligand binding domain). Indeed, previous X-ray co-crystal study of the complexes between hVDR-LBD and TPD-006, a hydrogen bond formation between the oxygen atom cyclopentanone and His397 was observed [58]. Derivatives having the dimethyl groups on the cyclopentanone moiety would greatly increase lipophilicity and VDR activities (TPD-003, TPD-005, TPD-006, TPD-008 and TPD-009), hence strong activities with the GAL4-hVDR assay (Fig. 8; Table 3). In the VDR-LBD, the terminal side chain of ligand is located in the lipophilic region [42], and lipophilicity of the dimethyl groups would contribute to higher activities. When we evaluated derivatives that were modified at C-2 position, such as 2-methylene group (TPD-008 and TPD-009) and 2-hydroxypropyloxy group (TPD-005, TPD-006, TPD-007), we observed enhancement of transactivation activities, again verified by the GAL4 assay (Table 3). TPD-004, which is a 3-epi-analog that differs from TPD-003 only in the stereochemistry of the C-3 hydroxyl group (left side hydroxyl group), its activity is drastically reduced, whereas for TPD-009, which is a 14-epimer of TPD-008, there was only a slight decrease in transactivation activity. The stereochemistry of the hydroxyl group is therefore important for binding to the VDR and transactivation activity.

Regarding the straight side chain derivatives, we found that TPD-012 displayed much decreased activity. For this compound, substitution of the 3-epi-hydroxy group and 25-fluorine groups greatly decreased activity due to loss of binding to the VDR active site. TPD-013 also showed decreased transactivation activity, although it was reported that this compound showed same transactivation activity as that of $1,25(OH)_3D_3$ in Hos cells [59]. It was reported that introduction of hydroxyalkyl group/hydroxyalkoxy group to C-2 group enhanced their biological activities by formation of hydrogen bond with Arg274 in VDR-LBD [60]. However, the previous X-ray co-crystal study of the complexes between this compound and hVDR-LBD showed other hydrogen bond formation, but not with Arg274 but Asp144 [59]. We surmise that the difference in hydrogen bond formation and in different cell types affected the EC_{50} values in transactivation activity. The lactone ring derivatives of $1,25(OH)_2D_3$, TPD-014 and TPD-090, are both less potent at inducing human VDR than $1,25(OH)_2D_3$. In fact, TPD-014, also known as TEI-9647, and TPD-090 both belong to a class of 1α,25-dihydroxyvitamin D_3-26–23 lactones known to be VDR antagonists [31]. The antagonistic effects are confirmed by inhibition of differentiation of HL-60 cells, pagetic bone marrow cells, osteoclasts formation [61–65], and calcium transport and mobilization [66]. Antagonism exists due to either the weaker interaction between the VDR and RXRα [62], or to a unique non-covalent conformational change [67].

Excluding the antagonists, TPD-014 and TPD-090, a few lead compounds could be identified in our luciferase assay in HEK293 cells (TPD-001-TPD-009) (Fig. 8). Our screens revealed that most of the TPD compounds induced CYP24A1 but not necessarily MDR1 in hCMEC/D3 cells; only TPD-003, TPD-004, TPD-013, and TPD-014, showed significant increases in MDR1 mRNA expression (Fig. 9). The desirability for TPD-003 and TPD-004 was dampened since these are strong inducers of TRPV6 in Caco-2 cells and only TPD-090 and TPD-002 showed the lowest induction of TRPV6 mRNA expression (Fig. 10E). All other TPD compounds caused large induction of TRPV6 in Caco-2 cells, again suggesting hypercalcemia. TPD-002, however, is not a good candidate since the increase in MDR1 in hCMEC/D3 was not significant (Fig. 9B).

Our work emphasizes the limitations of cell-based systems and the need for enzyme inhibitors such as KTZ, which when absent, would distort the true potency estimates and inductive potentials expected of intact VDRAs and VDRMs (Figs. 1 and 5). By contrast, absence of the metabolic inhibitor could provide vital information as to potential for bioactivation in vivo [28]. With the improved systems, the search continues to find other suitable VDR agonist that could retain all positive effects of $1,25(OH)_2D_3$ without eliciting hypercalcemia.

5. Authorship

PB carried out the transfection and GAL4-hVDR potency studies in HEK293 cells with the precursor compounds and the VDRAs from Teijin Pharma, conducted experiments on the hCMEC/D3 and Caco-2 cells, and prepared the draft of the paper. HS synthesized the Teijin VDRAs and contributed to comments on SAR of the Teijin compounds. LM carried out the incubation studies of HEK293 with VDRAs and prepared samples for the $1,25(OH)_2D_3$ EIA assay and contributed to the discussion on activity of the Teijin compounds. ECC carried out the EIA assay for $1,25(OH)_2D_3$. CLC designed the experiments for HEK293 cells and contributed to the writing of the manuscript. APL provided human proximal cells and human liver tissue as standards for comparison of enzyme relative protein levels in renal cells. KSP performed the simulations of data, with and without KTZ, on the formation of active $1,25(OH)_2D_3$ to predict RLU associated with $25(OH)D_3$ or $1α(OH)D_3$ and $1,25(OH)_2D_3$, designed the KTZ experiments, and contributed to the writing of the manuscript.

6. Conflict of interest

The authors declare no conflicts of interest related to this manuscript.

Acknowledgements

This work was supported by research grants from the Canadian Institutes for Health Research (CIHR) (KSP), a training grant from CIHR (PB), and Center for Collaborative Drug Research (CCDR), Department of Pharmacology, University of Toronto (KSP). We thank Dr. Rommel G. Tirona, University of Western Ontario, for providing the standard for the purchased, human kidney homogenate.

References

[1] Y. Tanaka, H.F. DeLuca, Rat renal 25-hydroxyvitamin D_3 1- and 24-hydroxylases: their in vivo regulation, Am. J. Physiol. 246 (1984) E168–E173.
[2] J.B. Cheng, D.L. Motola, D.J. Mangelsdorf, D.W. Russell, De-orphanization of cytochrome P450 2R1: a microsomal vitamin D 25-hydroxilase, J. Biol. Chem. 278 (2003) 38084–38093.
[3] R.P. Gupta, B.W. Hollis, S.B. Pate, K.S. Patrick, N.H. Bell, CYP3A4 is a human microsomal vitamin D 25-hydroxylase, J. Bone Miner. Res. 19 (2004) 680–688.
[4] B.W. Hollis, Assessment of vitamin D nutritional and hormonal status: what to measure and how to do it, Cal. Tissue Int. 58 (1996) 4–5.
[5] H.F. Deluca, J.M. Prahl, L.A. Plum, 1,25-Dihydroxyvitamin D_3 is not responsible for toxicity caused by vitamin D or 25-hydroxyvitamin D, Arch. Biochem. Biophys. 505 (2011) 226–230.
[6] G. Jones, S.A. Strugnel, H.F. DeLuca, Current understanding of the molecular actions of vitamin D, Physiol. Rev. 78 (1998) 1193–1231.
[7] E. den Dekker, J.G. Hoenderop, B. Nilius, R.J. Bindels, The epithelial calcium channels, TRPV5 & TRPV6: from identification towards regulation, Cell Calcium. 33 (2003) 497–507.
[8] Q.J. Yang, P. Bukuroshi, H.P. Quach, E.C.Y. Chow, K.S. Pang, Highlighting vitamin D receptor-targeted activities of 1α,25-dihydroxyvitamin D_3 in mice via physiologically based pharmacokinetic-pharmacodynamic modeling, Drug Metab. Dispos. 46 (2018) 75–87.
[9] E.C. Chow, M. Sondervan, C. Jin, G.M. Groothuis, K.S. Pang, Comparative effects of doxercalciferol (1α-hydroxyvitamin D_2) versus calcitriol (1α,25-dihydroxyvitamin D_3) on the expression of transporters and enzymes in the rat in vivo, J. Pharm. Sci. 100 (2011) 1594–1604.
[10] J.J. Eloranta, C. Hiller, M. Juttner, G.A. Kullak-Ublick, The SLCO1A2 gene, encoding human organic anion-transporting polypeptide 1A2, is transactivated by the vitamin D receptor, Mol. Pharmacol. 82 (2012) 37–46.
[11] Y.C. Kim, I.B. Kim, C.K. Noh, H.P. Quach, I.S. Yoon, E.C.Y. Chow, et al., Effects of 1α,25-dihydroxyvitamin D_3, the natural vitamin D receptor ligand, on the pharmacokinetics of cefdinir and cefadroxil, organic anion transporter substrates, in rat, J. Pharm. Sci. 103 (2014) 3793–3805.
[12] H.P. Quach, K. Noh, S.Y. Hoi, A. Bruinsma, G.M.M. Groothuis, A.P. Li, et al., Alterations in gene expression in vitamin D-deficiency: down-regulation of liver Cyp7a1 and renal Oat3 in mice, Biopharm. Drug Dispos. 39 (2018) 99–115.
[13] I. Echchgadda, C.S. Song, A.K. Roy, B. Chatterjee, Dehydroepiandrosterone sulfotransferase is a target for transcriptional induction by the vitamin D receptor, Mol. Pharmacol. 65 (2004) 720–729.
[14] P. Schmiedlin-Ren, K.E. Thummel, J.M. Fishe, M.F. Paine, W.B. Watkins, Induction of CYP3A4 by 1α,25-dihydroxyvitamin D_3 is human cell line-specific and is unlikely to involve pregnane X receptor, Drug Metab. Dispos. 29 (2001) 1446–1453.
[15] K. Inouye, T. Sakaki, Enzymatic studies on key enzymes of vitamin D metabolism; 1α-hydroxylase (CYP27B1) and 24-hydroxylase (CYP24), Biotechnol. Annu. Rev. 7 (2001) 179–194 (ed. M.R. El-Gewely).
[16] T. Wong, Z. Wang, B.D. Chapron, M. Suzuki, K.G. Claw, C. Gao, R.S. Foti, et al., Polymorphic human sulfotransferase 2A1 mediates the formation of 25-hydroxyvitamin D_3-3-O-sulfate, a major circulating vitamin D metabolite in humans, Drug Metab. Dispos. 46 (2018) 367–379.
[17] C. Gao, M.C. Bergagnini-Kolev, M.Z. Liao, Z. Wang, T. Wong, J.C. Calamia, et al., Simultaneous quantification of 25-hydroxyvitamin D_3-3-sulfate and 25-hydroxyvitamin D_3-3-glucuronide in human serum and plasma using liquid chromatography-tandem mass spectrometry coupled with DAPTAD-derivatization, J. Chromatogr. B Analyt. Technol. Biomed. Life Sci. 1060 (2017) 158–165.
[18] C.P. Hawkes, D. Li, H. Hakonarson, K.E. Meyers, K.E. Thummel, M.A. Levine,

CYP3A4 induction by rifampin: an alternative pathway for vitamin D inactivation in patients with CYP24A1, J. Clin. Endocrinol. Metab. 102 (2017) 1440–1446.
[19] Z. Wang, T. Wong, T. Hashizume, L.Z. Dickmann, M. Scian, N.J. Koszewski, J.P. Goff, et al., Human UGT1A4 and UGT1A3 conjugate 25-hydroxyvitamin D_3: metabolite structure, kinetics, inducibility, and interindividual variability, Endocrinology 155 (2014) 2052–2063.
[20] Z. Wang, Y.S. Lin, L.J. Dickmann, E.J. Poulton, D.L. Eaton, J.W. Lampe, D.D. Shen, et al., Enhancement of hepatic 4-hydroxylation of 25-hydroxyvitamin D_3 through CYP3A4 induction in vitro and in vivo: implications for drug-induced osteomalacia, J. Bone Miner. Res. 28 (2013) 1101–1116.
[21] R. Vieth, K. McCarten, K.H. Norwich, Role of 25-hydroxyvitamin D_3 dose in determining rat 1,25-dihydroxyvitamin D_3 production, Am. J. Physiol. 258 (1990) E780–E789.
[22] Z.G. Zhu, J.T. Ochalek, M. Kaufmann, G. Jones, H.F. Deluca, CYP2R1 is a major, but not exclusive, contributor to 25-hydroxyvitamin D production in vivo, Proc. Natl Acad. ScI. U.S.A. 110 (2013) 15650–15655.
[23] T.D. Thacher, P.R. Fischer, R.J. Singh, J. Roizen, M.A. Levine, *CYP2R1* mutations impair generation of 25-hydroxyvitamin D and cause an atypical form of vitamin D deficiency, J. Clin. Endocrinol. Metab. 100 (2015) E1005–E1013.
[24] Y. Ohyama, K. Okuda, Isolation and characterization of a cytochrome P-450 from rat kidney mitochondria that catalyzes the 24-hydroxylation of 25-hydroxyvitamin D_3, J. Biol. Chem. 266 (1991) 8690–8695.
[25] E.C. Chow, M.R. Durk, H.J. Maeng, K.S. Pang, Comparative effects of 1α-hydroxyvitamin D_3 and 1,25-dihydroxyvitamin D_3 on transporters and enzymes in *fxr*(+/+) and *fxr*(−/−) mice, Biopharm. Drug Dispos. 34 (2013) 402–416.
[26] J. Fan, S. Liu, Y. Du, J. Morrison, R. Shipman, K.S. Pang, Up-regulation of transporters and enzymes by the vitamin D receptor ligands, 1α,25-dihydroxyvitamin D_3 and vitamin D analogs, in the Caco-2 cell monolayer, J. Pharmacol. Exp. Ther. 330 (2009) 389–402.
[27] S. Nishida, J. Ozeki, M. Makishima, Modulation of bile acid metabolism by 1α-hydroxyvitamin D_3 administration in mice, Drug Metab. Dispos. 37 (2009) 2037–2044.
[28] H.P. Quach, T. Dzekic, P. Bukuroshi, K.S. Pang, Potencies of vitamin D analogs, 1α-hydroxyvitamin D_3, 1α-hydroxyvitamin D_2, and 25-hydroxyvitamin D_3, in lowering cholesterol in hypercholesterolemic mice in vivo, Biopharm. Drug Dispos. 39 (2018) 196–204.
[29] M.R. Durk, K. Han, E.C. Chow, R. Ahrens, J.T. Henderson, P.E. Fraser, K.S. Pang, 1α,25-Dihydroxyvitamin D_3 reduces cerebral amyloid-beta accumulation and improves cognition in mouse models of Alzheimer's disease, J. Neurosci. 34 (2014) 7091–7101.
[30] K. Ozono, M. Saito, F. Miura, T. Michigami, S. Nakajima, S. Ishizuka, Analysis of the molecular mechanism for the antagonistic action of a novel 1α,25-dihydroxyvitamin D_3 analogue toward vitamin D receptor function, J. Biol. Chem. 274 (1999) 32376–32381.
[31] A. Toel, M.M. Gonzalez, D. Ruf, A. Steinmeyer, S. Ishizuka, C. Carlberg, Different molecular mechanisms of vitamin D_3 receptor antagonists, Mol. Pharmacol. 59 (2001) 1478–1485.
[32] S. Ishizuka, S. Ishimoto, A.W. Norman, Isolation and identification of 1α,25-dihydroxy-24-oxovitamin D_3, 1α,25-dihydroxyvitamin D_3 26,23-lactone, and 1α,25,24(S),25-trihydroxyvitamin D_3: in vivo metabolites of 1α,25-dihydroxyvitamin D_3, Biochemistry 23 (1984) 1473–1478.
[33] M.B. Meyer, L.A. Zella, R.D. Nerenz, J.W. Pike, Characterizing early events associated with the activation of target genes by 1,25-dihydroxyvitamin D_3 in mouse kidney and intestine in vivo, J. Biol. Chem. 282 (2007) 22344–22352.
[34] R. Adachi, A.I. Shulman, K. Yamamoto, I. Shimomura, S. Yamada, D.J. Mangelsdorf, et al., Structural determinants for vitamin D receptor response to endocrine and xenobiotic signals, Mol. Endocrinol. 18 (2004) 43–52.
[35] E.C. Chow, H.P. Quach, R. Vieth, K.S. Pang, Temporal changes in tissue 1α,25-dihydroxyvitamin D_3, vitamin D receptor target genes, and calcium and PTH levels after $1,25(OH)_2D_3$ treatment in mice, Am. J. Physiol. Endocrinol. Metab. 304 (2013) E977–E989.
[36] E.C. Chow, L. Magomedova, H.P. Quach, R. Patel, M.R. Durk, J. Fan, et al., Vitamin D receptor activation down-regulates the small heterodimer partner and increases CYP7A1 to lower cholesterol, Gastroenterology 146 (2014) 1048–1059.
[37] M.R. Durk, G.N. Chan, C.R. Campo, J.C. Peart, E.C. Chow, E. Lee, et al., 1α,25-Dihydroxyvitamin D_3-liganded vitamin D receptor increases expression and transport activity of P-glycoprotein in isolated rat brain capillaries and human and rat brain microvessel endothelial cells, J. Neurochem. 123 (2012) 944–953.
[38] O.H. Lowry, M.J. Rosebrough, A.L. Farr, R.J. Randall, Protein measurement with the Folin phenol reagent, J. Biol. Chem. 193 (1951) 265–275.
[39] T. Aiba, M. Susa, S. Fukumori, Y. Hashimoto, The effects of culture conditions on CYP3A4 and MDR1 mRNA induction by 1α,25-dihydroxyvitamin D_3 in human intestinal cell lines, Caco-2 and LS180, Drug Metab. Pharmacokinet. 20 (2005) 268–274.
[40] L. Asano, I. Ito, N. Kuwabara, T. Waku, J. Yanagisawa, H. Miyauchi, T. Shimizu, Structural basis for vitamin D receptor agnoism by nonvel non-secosteroidal ligands, FEBS Lett. 587 (2013) 957–963.
[41] S.A. Khedkar, M.A. Samad, S. Choudhury, L.Y. Lee, D. Zhang, R.I. Thadhani, et al., Identification of novel non-secosteroidal vitamin D receptor agonists with potent cardioprotective effects and devoid of hypercalcemia, Sci. Rep. 7 (1) (2017) 8427.
[42] S. Hourai, L.C. Rodrigues, P. Antony, B. Reina-San-Martin, F. Ciesielski, B.C. Magnier, et al., Structure-based design of a superagonist ligand for the vitamin D nuclear receptor, Chem. Biol. 15 (2008) 383–392.
[43] M. Herdick, A. Steinmeyer, C. Carlberg, Antagonistic action of a 25-carboxylic ester analogue of 1α,25-dihydroxyvitamin D_3 is mediated by a lack of ligand-induced vitamin D receptor interaction with coactivators, J. Biol. Chem. 275 (2000) 16506–16512.
[44] A.R. Giuliano, R.J. Wood, Vitamin D-regulated calcium transport in Caco-2 cells: unique in vitro model, Am. J. Physiol. 260 (1991) G207–G212.
[45] M.V. Chirayath, L. Gajdzik, W. Hull, J. Graf, H.S. Cross, M. Peterlik, Vitamin D increases tight-junction conductance and paracellular Ca2+ transport in Caco-2 cell cultures, Am. J. Physiol. 27 (1998) G389–G396.
[46] K. El Abdaimi, V. Papavasiliou, S.A. Rabbani, J.S. Rhim, F. Goltzman, R. Kremer, Reversal of hypercalcemia with the vitamin D analogue EB1089 in a human model of squamous cancer, Cancer Res. 59 (1999) 3325–3328.
[47] J.C. Fleet, F. Eksir, K.W. Hance, R.J. Wood, Vitamin D-inducible calcium transport and gene expression in three Caco-2 cell lines, Am. J. Physiol. Gastrointest. Liver Physiol. 283 (2002) G618–G625.
[48] M.B. Meyer, M. Watanuki, S. Kim, N.K. Shevde, J.W. Pike, The human transient receptor potential vanilloid type 6 distal promoter contains multiple vitamin D receptor binding sites that mediate activation by 1,25-dihydroxyvitamin D_3 in intestinal cells, Molec. Endocrinol. 20 (2006) 1447–1461.
[49] J.G. Hoenderop, A.W. van der Kemp, A. Hartog, S.F. van de Graaf, C.H. van Os, P.H. Willems, et al., Molecular identification of the apical Ca2+ channel in 1,25-dihydroxyvitamin D_3-responsive epithelia, J. Biol. Chem. 274 (1999) 8375–8378.
[50] A. Fukushima, Y. Aizaki, K. Sakuma, Short-chain fatty acids induce intestinal transient receptor potential vanilloid type 6 expression in rats and Caco-2 cells, J. Nutrit. 139 (2009) 20–25.
[51] J. Inoue, J.M. Choi, T. Yoshidomi, T. Yashiro, R. Sato, Quercetin enhances VDR activity, leading to stimulation of its target gene expression in Caco-2 cells, J. Nutrit. Sci. Vitaminol. 56 (2010) 326–330.
[52] S. Dauchy, F. Miller, P.O. Couraud, R.J. Weaver, B. Weksler, I.A. Romero, et al., Expression and transcriptional regulation of ABC transporters and cytochromes P450 in hCMEC/D3 human cerebral microvascular endothelial cells, Biochem. Pharmacol. 77 (2009) 897–909.
[53] O. Huber, A. Brunner, P. Maier, R. Kaufmann, P.O. Couraud, C. Creme, et al., Localization microscopy (SPDM) reveals clustered formations of P-glycoprotein in a human blood-brain barrier model, PloS One 7 (2012) e44776.
[54] S. Takeda, Y. Kitajima, Y. Ishii, Y. Nishimura, P.I. Mackenzie, K. Oguri, et al., Inhibition of UDP-glucuronosyltransferase 2B7-catalyzed morphine glucuronidation by ketoconazole: dual mechanisms involving a novel noncompetitive mode. Short Communication, Drug Metab. Dispos. 34 (2006) 1277–1282.
[55] Y. Liu, M. She, Z. Wu, R. Dai, The inhibition study of human UDP-glucuronsyltransferases with cytochrome 450 selective substrates and inhbitors, J. Enzyme Inhibit. Med. Chem. 16 (2011) 386–393.
[56] J. Trachtenberg, J. Zadra, Steroid synthesis inhibition by ketoconazole: sites of action, Clin. Investig. Med. 11 (1988) 1–5.
[57] J.W. Mueller, L.C. Gilligan, J. Idkowiak, W. Arlt, P.A. Foster, The regulation of steroid action by sulfation and desulfation, Endocrinol. Rev. 36 (2015) 526–563.
[58] H. Saitoh, K. Takagi, K. Horie, S. Kakuda, M. Takimoto-Kamimura, E. Ochiai, et al., Synthesis of novel C-2 substituted vitamin D derivatives having ringed side chains and their biological evaluation on bone, J. Steroid Biochem. Mol. Biol. 136 (2013) 3–8.
[59] H. Saitoh, K. Watanabe, S. Kakuda, M. Takimoto-Kamimura, K. Takagi, et al., Synthesis and biological activities of vitamin D_3 derivatives with cycloalkyl side chain at C-2 position, J. Steroid Biochem. Mol. Biol. 148 (2015) 27–30.
[60] S. Hourai, T. Fujishima, A. Kittaka, Y. Suhara, H. Takayama, et al., Probing a water channel near the A-ring of receptor – bound 1α,25-dihydroxyvitamin D_3 with selected 2α-substituted analogues, J. Biol. Chem. 49 (2006) 5199.
[61] D. Miura, K. Manabe, K. Ozono, M. Saito, Q. Gao, A.W. Norman, et al., Antagonistic action of novel 1α,25-dihydroxyvitamin D_3-26,23-lactone analogs on differentiation of human leukemia cells (HL-60) induced by 1α,25-dihydroxyvitamin D_3, J. Biol. Chem. 274 (1999) 16392–16399.
[62] K. Ozono, M. Saito, D. Miura, T. Michigami, S. Nakajima, S. Ishizuka, Analysis of the molecular mechanism for the antagonistic action of a novel 1α,25-dihydroxyvitamin D_3 analogue toward vitamin D receptor function, J. Biol. Chem. 274 (1999) 32376–32381.
[63] S. Ishizuka, N. Kurihara, D. Miura, K. Takenouchi, J. Cornish, T. Cundy, et al., Vitamin D antagonist, TEI-9647, inhibits osteoclast formation induced by 1α,25-dihydroxyvitamin D_3 from pagetic bone marrow cells, J. Steroid Biochem. Mol. Biol. 89–90 (2004) 331–334.
[64] S. Ishizuka, N. Kurihara, S.W. Reddy, J. Cornish, T. Cundy, G.D. Roodman, (23S)-25-Dehydro-1α-hydroxyvitamin D_3-26,23-lactone, a vitamin D receptor antagonist that inhibits osteoclast formation and bone resorption in bone marrow cultures from patients with Paget's disease, Endocrinology 146 (2005) 2023–2030.
[65] S. Ishizuka, N. Kurihara, Y. Hiruma, D. Miura, J.-L. Namekawa, A. Tamura, et al., 1α,25-Dihydroxyvitamin D_3–26,23-lactam analogues function as vitamin D receptor antagonists in human and rodent cell, J. Steroid Biochem. Mol. Biol. 110

(2008) 269–277.
[66] S. Ishizuka, D. Miura, K. Ozono, M. Chokki, H. Mimura, A.W. Norman, Antagonistic actions in vivo of (23S)-25-dehydro-1α-hydroxyvitamin D_3–26,23-lactone on calcium metabolism induced by 1α,25-dihydroxyvitamin D_3, Endocrinology 142 (2001) 59–67.
[67] C.M. Bula, J.E. Bishop, S. Ishizuka, A.W. Norman, 25-Dehydro-1α-hydroxyvitamin D_3–26,23S-lactone antagonizes the nuclear vitamin D receptor by mediating a unique noncovalent conformational change, Molec. Endocrinol. 14 (2000) 1788–1796.

Glossary

1α(OH)D_3: 1α-hydroxyvitamin D_3
1,25(OH)$_2$D$_3$: 1α,25-dihydroxyvitamin D_3
25(OH)D_3: 25-hydroxyvitamin D_3
CYP2R1: human liver microsomal enzyme for formation of 25(OH)D_3 from vitamin D_3
CYP24A1: human degradation enzyme of 1,25(OH)$_2$D$_3$
CYP27A1: human liver mitochondrial enzyme for formation of 25(OH)D_3 from vitamin D_3
CYP27B1: human liver mitochondrial enzyme for formation of 1,25(OH)$_2$D$_3$ from 25(OH)D_3
CYP3A4: human cytochrome P450 enzyme 3A4
EC_{50}: concentration at 50% of maximum activation
E_{max}: maximum response
FXR: human farnesoid X receptor
GAPDH: human glyceraldehyde-3-phosphate dehydrogenase
KTZ: ketoconazole
LDH: lactate dehydrogenase
MDR1: human multidrug resistance protein 1
MRP: human multidrug resistance-associated protein
OATP1A2: human organic anion-transporting polypeptide
P-gp: P-glycoprotein
qPCR: quantitative real-time polymerase chain reaction
RLU: relative luciferase units
SDS: sodium dodecyl sulfate
SULT2A1: human sulfotransferase 2A1
TRPV: human transient receptor potential vanilloid channel
TPD: Teijin vitamin D receptor analog
VDR: human vitamin D receptor
VDRA: vitamin D receptor activator
VDRE: human vitamin D response element